

5-2009

Reliability of Light Frame Roof Systems Subject to High Winds

Angelina Gleason

Clemson University, angelig@clemson.edu

Follow this and additional works at: https://tigerprints.clemson.edu/all_theses



Part of the [Civil Engineering Commons](#)

Recommended Citation

Gleason, Angelina, "Reliability of Light Frame Roof Systems Subject to High Winds" (2009). *All Theses*. 554.
https://tigerprints.clemson.edu/all_theses/554

This Thesis is brought to you for free and open access by the Theses at TigerPrints. It has been accepted for inclusion in All Theses by an authorized administrator of TigerPrints. For more information, please contact kokeefe@clemson.edu.

RELIABILITY OF LIGHT FRAME ROOF SYSTEMS SUBJECT TO HIGH
WINDS

A Masters Thesis
Presented to
the Graduate School of
Clemson University

in Partial Fulfillment
of the Requirements for the Degree
Master of Science
Civil Engineering

by
Angelina Victoria Gleason
May 2009

Accepted by:
Dr. Bryant G. Nielson, Committee Chair
Dr. Nigel B. Kaye
Dr. WeiChiang Pang

ABSTRACT

Recent hurricane damages have devastated coastal communities and focused national attention on hurricane damage mitigation. Structural damage is one of the most significant impacts of a hurricane. Even small levels of structural damage can result in large economic losses; when gaps open in the roof system, rain water can leak in, ruining the contents of the structure and rendering it uninhabitable although it is still standing. In order to prevent these secondary damages from occurring, a better understanding of the roof system behavior is essential. This research aims to ascertain the behavior of the roof system by determining the influence of variable stiffness in the roof-to-wall connection on system behavior and to develop and propose a method for determining the reliability of a roof system typical to low-rise residential wood construction under wind loads.

Monte Carlo simulations were run on a computer model of the roof system using probability density functions for both structural parameters and load variables. The goal of these simulations was to determine the effect of variable connection stiffness and wind zone discretization on the reliability of the roof system. One significant development this study utilized was an analytical connection model for the roof-to-wall connection, capable of shedding load past a randomly generated capacity value, taken from previous research. Sheathing wind loads were modeled as a lognormal variable and generated within the constraints of a correlation matrix.

Results were obtained utilizing this Monte Carlo simulation. The system reliability was calculated as approximately 0.95 for a wind speed of 100 mph and 0.62 for a wind speed of 130 mph. The study's results suggested that considering the variability in connection stiffness had little effect on the system reliability. The level of correlation between pressures on the roof, however, was shown to have a significant effect on the system reliability.

ACKNOWLEDGEMENTS

I would like to express my sincere appreciation for the guidance my committee chair, Dr. Bryant G. Nielson, has provided to me throughout my work on this document. His enthusiasm, knowledge and consistently positive attitude kept me going throughout not only my graduate work, but my undergraduate program as well.

Thanks to my parents, John and Linda Gleason, for their unconditional support, both emotionally and financially, in pursuing an advanced degree and every other aspect of my life. This thesis would not have been possible without them.

I would also like to thank my fiancé, Jerry Stasulis, for spending hours reading and commenting up countless drafts of a thesis in an area in which he has no expertise. His willingness to learn what I was doing and help me achieve my goals is greatly appreciated.

I would also like to acknowledge the work done by Michigan Tech's Yue-Jun Yin on the windPRESSURE correlation matrix in his unpublished paper "Correlation Coefficients Matrix for Wind Pressure Coefficients". This paper served as a basis for the correlation matrix utilized in this study.

TABLE OF CONTENTS

	Page
TITLE PAGE	i
ABSTRACT.....	ii
ACKNOWLEDGEMENTS.....	iv
LIST OF TABLES	vii
LIST OF FIGURES.....	viii
CHAPTER	
1. INTRODUCTION	1
2. LITERATURE REVIEW.....	4
Introduction.....	4
Wind Induced Structural Damage	5
Experimental Studies	6
Analytical Studies.....	8
Reliability Analyses.....	9
System Behavior	10
3. MODEL.....	12
Base Structure	12
Modeling Medium.....	13

Table of Contents (Continued)

Structural Model.....	14
Roof-to-wall Connection Model	18
Load Distribution	21
Model Verification	22
4. WIND LOADS	29
Wind Behavior	29
Wind Loads.....	31
Modeling Methods	34
Modeling Approach.....	37
Load Application.....	46
5. RELIABILITY	47
Fundamentals of Reliability	47
Monte Carlo Simulation	49
Load Scenarios	50
Simulation Procedure	52
Results.....	53
Evaluation of Accuracy	59
Fragility Curves.....	61
6. CONCLUSIONS	63
Effect of Variable Stiffness on System Reliability	63
Proposed Method for Evaluating System Reliability	64
Recommendations for Future Work	65
REFERENCES.....	69

LIST OF TABLES

Table		Page
3.1	Probability distributions for analytical connection model.....	20
4.1	Wind load distribution parameters	38
5.1	Simulation summary.....	51
5.2	Probabilities of failure	54
5.3	Ratio of failed connections in failed realizations	58
5.4	Proportion of connections within five percent of failure in failed realizations	59
5.5	Median wind speeds	62

LIST OF FIGURES

Figure	Page
3.1 Douhit Hills Structure.....	12
3.2 Detail of actual connection	13
3.3 Assumed location of trusses in this study.....	15
3.4 Rendering of model	16
3.5 Assignment of tributary properties to sheathing beams	17
3.6 Truss Model	18
3.7 Force-displacement behavior of analytical connection model.....	19
3.8 Effect of sheathing stiffness on load distribution.....	24
3.9 System fragility curves for different exposure categories	26
3.10 Connection failure propagation under uniform load	27
4.1 Velocity profiles and boundary layers for laminar and turbulent flows.....	30
4.2 Effect of obstructions on wind velocity.....	31
4.3 Spectrum of horizontal wind speed	33
4.4 Wind flow around a structure.....	34
4.5 Wind zones used for method 2 calculations.....	35
4.6 Components and cladding wind zones	36
4.7 Sub-region locations	39
4.8 Median wind pressures (in psf) for 100 mph wind speed.....	39

List of Figures (continued)

Figure	Page
4.9 Median wind pressures (in psf) for 130 mph wind speed.....	40
4.10 Top view of wind direction.....	41
4.11 Building model with taps by windPRESSURE	42
4.12 Development of correlation equation	43
4.13 Excerpt from correlation matrix.....	44
4.14 Correlation contours for all panels relative to panel 1.....	44
4.15 Sample wind realization with panel correlation #1	45
4.16 Sample wind realization with panel correlation #2.....	45
5.1 Typical convergence of probability estimate with increasing sample size...50	
5.2 Conditional probabilities of failure	57
5.3 Probability of failure versus number of realizations	60-61
5.4 Extrapolated fragility curve (illustration only)	62
6.1 Fragility curves for multiple limit states (illustration only).....	67

CHAPTER ONE

INTRODUCTION

The response of low-rise wood frame (LRWF) roof structures subject to wind uplift is problematic. Structures are not designed to be indestructible, but some level of damage mitigation is expected from occupants and owners. Attempting to design an infallible building would be entirely too expensive and impractical. Furthermore, such a task would be impossible, since design loads would have been based on past experiences, and it is possible that the maximum extreme wind event, a hurricane, has not yet occurred. Designs are made based on code-level loads, which are generated with some consideration to the probability of various events occurring over the lifetime of the structure.

For economy, current building codes do not attempt to prevent damage to the structure under extreme events. The code aims for zero damage under normal working conditions, some nonstructural damage under moderately intense events, and strives to maintain life safety in extreme events. The design values corresponding to each of these conditions were derived from reliability studies, which measure the probability of failure of a system given certain conditions, such as a return period. Reliability analyses assist in determining appropriate design limits so that the probability of failure can be set to an appropriate limit.

Since this concept, known as performance-based engineering, is relatively new, many existing structures were not designed according to this methodology. As a result,

there is limited knowledge about the performance of these structures and their expected probability of failure. Recent hurricane events have devastated coastal communities and focused national attention on hurricane damage mitigation. Of particular concern is the excessive amount of damage occurring to the roofs of residential structures (Pielke 2008). It is believed that much of the existing construction in hurricane-prone regions possesses details similar to those used in the 1950s-60s. In order to prevent excessive damages from occurring in future storms, a better understanding of the roof system behavior is essential.

The response of a structure is governed by its material properties, the interactions of the structural members (load path), and loads applied unto it. For a wooden roof truss system under wind load, these values are highly variable. Wood, as a material, has a high degree of variability due to different species, moisture contents, grain patterns and sizes. As the material properties change, so does the response of the structure. The load path is influenced by the connections between the members, particularly the roof-to-wall connection. Variability in construction techniques, connection type and materials used can dramatically change the behavior of the roof-to-wall connection, impacting the load distribution path.

There is a host of variables to consider when determining the structural response to wind load. Temporal and spatial variations in wind velocity, a result of turbulence, make modeling the wind load difficult. Since these variations are not completely random, some sort of correlation constraints must be used in generating a load model. Within the structure, material variability and inherent differences in construction techniques cause additional complexities. The variability in the behavior of the toe-nailed roof-to-wall

connection is one significant influence on the structural response. The inherent inconsistency in field construction practices for the roof-to-wall connection affects the amount of load carried by each connection and the way in which load is redistributed to surviving connections after a single connection failure. Addressing this variability may show that system failure is not imminent given the failure of a single connection and can thus appropriately capture system effects of load redistribution.

This research aims to ascertain the behavior of a typical light-frame roof system and present its performance in terms of a system reliability. Objectives of this research include:

- To determine the influence of inherent variability in the properties of key components on roof system behavior
- To develop and propose an enhanced method for determining the reliability of a roof system typical to low-rise residential wood construction under wind loads. In particular, special effort is made to account for system effects.

The remaining chapters of this thesis provide deeper discussion on the current state of the problem, modeling procedures, analysis methods and conclusions drawn. Chapter 2 discusses additional information about current and past research pertinent to this investigation. Chapter 3 focuses on the development and usage of the computer model utilized in the analysis. Chapter 4 provides a discussion of wind load modeling methods used. Chapter 5 explains the reliability analysis performed. Conclusions about the behavior of the roof system are made in Chapter 6.

CHAPTER TWO

LITERATURE REVIEW

Introduction

Natural disasters have always been a threat to mankind. Hurricanes are the most devastating of these events, as their damage comes in multiple forms. Massive amounts of rain floods buildings and roads, storm surge erodes shorelines and flood inland areas, and high winds destroy structures of all types. Within the past century, the United States has been hit by over 150 hurricanes and will certainly experience many more{{59 Blake, Eric S. 2007}}.

In 2005, Hurricane Katrina made headlines around the world as one of the worst natural disasters in history with \$81 billion in damage along the Gulf Coast (Blake et al. 2007). Government, insurance and other officials were forced to investigate why existing preparations had been insufficient and what was necessary to avoid a recurrence. One theory was that global climate changes may be causing stronger hurricanes, but the intensity of recent storms is not unprecedented (Pielke and Landsea 1998). The significant increase in damage is due to the population growth and development in hurricane-prone areas, and not an increase in hurricane strength (Jarrell et al. 2001; Davidson et al. 2003; Pinelli et al. 2004).

To encourage communities to be proactive in reducing their own damages from natural disasters, FEMA has created a software program called HAZUS-MH (FEMA 2007). Though still in its early stages, this program is becoming widely used among

local government officials as a hazard management tool (Vickery et al. 2006). HAZUS-MH estimates the social and economic impact that a hurricane may impose on a given region. Included in this forecasting process are explicit estimations of the degree of damage to the built environment (Vickery et al. 2006). Other software programs account for variation in coastal development, structural retrofits and population growth (Davidson et al. 2003). All of these programs use inventory data and probabilistic methods to estimate the damage a community may incur over a particular time period. In essence, they aim to predict the probability and effects of a disaster.

Wind Induced Structural Damage

One of the most significant impacts of a hurricane is the structural damage caused by its high wind speeds (Sparks and Bhinderwala 1994). Although design provisions pertaining to wind loads exist, many buildings in the Gulf Coast were still total losses in Hurricane Katrina because not all structures are subject to such regulations (van de Lindt et al. 2007). The code governing a building's structural design depends on the building's usage and primary construction material. Industrial and commercial buildings, for example, are commonly governed by codes that reference ASCE 7: Minimum Design Loads for Buildings and Other Structures (van de Lindt et al. 2007, ASCE 2005). This specification aims to balance security with economy, by striving to facilitate a design that will maintain life-safety in extreme events, rather than complete infallibility. Many structures governed by this standard survived the wind loads (van de Lindt et al. 2007).

The majority of construction along America's hurricane-prone region, however, is not governed by the same code. Wood light-frame residential structures are often non-engineered, and thus not subject to the rules and regulations of ASCE 7 or other specifications dealing with hurricane wind forces. Structures falling into this category are constructed according to common practice and are not given any special design consideration. As a result, most of these structures failed under Katrina's winds (van de Lindt et al. 2007).

Post-Katrina investigations revealed several key failings of residential structures in the area (van de Lindt et al. 2007). Lack of uplift load path, inappropriate use of conventional construction procedures and poor attention to connection details were all causes of structural failures.

For residential structures, most hurricane-induced damage can be linked to roof failure (Reed, et al. 1997; Rosowsky et al. 1998; Cheng 2004). When a roof structure fails, water is allowed to enter, thereby ruining its interior and resulting in considerable damages (Sparks and Bhinderwala 1994). Because water damage is the leading source of hurricane-related insurance claims, this topic is of interest to homeowners and insurance companies alike (Keith and Rose 1994).

Experimental Studies

Over the past fifty years, wind loadings on low-rise wood construction have been the subject of many research projects. Particular focus has been given to the critical part of the roof system, identified as the top-plate to rafter connection (Reed, et al. 1997;

Rosowsky et al. 1998; Cheng 2004). Numerous studies have been done to develop capacities for the various types of structural connections at this location to assure that connections used have the strength necessary to resist the applied loadings.

Cheng (2004) tested the uplift capacities of toe-nail connections with various wood species, rafter sizes, nail sizes and nail schedules, chosen to reflect common construction practices. These capacities were then compared to the load demands calculated per ASCE 7-98 for various wind speeds (Cheng 2004). His tests, however, were all conducted per ASTM D 1761, which tests a single connection in an idealized environment (Cheng 2004). Even so, he concluded that nearly all of the connections would fail in a 90mph wind, the standard base wind for most of the country (American Society of Civil Engineers). For comparison, ASCE 7 stipulates a base wind of 110-120mph in hurricane-prone regions.

The results of idealized laboratory studies often lack practical application. Connection behavior of any system is not simply the combined behavior of its components (American Forest & Paper Association, Inc. 1993). The capacity of connections in a system is significantly higher than that of an independent connection, regardless of the type of connection (Rosowsky et al. 1998). The deviation of the system behavior from the cumulative component behavior is often referred to as a system effect.

Many research efforts have focused on determining the capacity for a roof system via full-size models. Roof shingles, insulation, membranes and other such components have little effect on the structural behavior of the system and are, consequently, neglected in the construction of such models. For simplicity, the roof system is often reduced to a

series of skeletal trusses (Reed et al. 1997; Rosowsky et al. 1998). Load is applied gradually with a hydraulic jack at the ASTM-specified loading rate to one connection. The system uplift capacity in these studies was taken to be load at which the connector pulls out, tears or the wood splits. This system capacity was divided by the number of connections to yield an “equivalent load” for comparison with the capacity of a stand-alone truss.

Analytical Studies

Connection capacities can be used in conjunction with a wind load to determine the probability the connection will fail. If the exact capacity of a connection and the load to be placed on it are known, the two values can easily be compared. For the critical rafter-to-top-plate connection, this is not the case. Both the connection strength and wind load can vary dramatically.

The strength of a connection is a function of the connector (toe-nail, strap, etc.), the properties of the wood used, and the method in which it is connected. To account for these variations, probabilistic distributions of connection properties have been developed from physical model analyses (Reed et al. 1997; Cheng 2004; Rosowsky et al. 1998; Shanmugam et al. 2009)

Design wind loads are typically calculated in accordance with ASCE 7 (ASCE 2005). The calculation method outlined in ASCE 7 yields a series of pressures that should be applied to various surfaces along the building envelope. However, these pressures are only valid for one particular storm event. Not every hurricane will exert identical forces

on a roof system. The values for a hurricane's intensity and the wind forces it generates are often modeled as probabilistic variables (Ellingwood et al. 2004; Ellingwood and Tekie 1999; Pourzeynali and Datta 2005). Statistical parameters for the distribution of the wind load are often based on a 1997 Delphi study conducted by Ellingwood and Tekkie (Cheng 2004; Ellingwood et al. 2004; Lee and Rosowsky 2005).

Reliability Analyses

Given public response to recent disasters, such as Hurricane Katrina, it has been suggested that design codes should be revised to facilitate performance-based design rather than simply strength design (Lee and Rosowsky 2005; Rosowsky and Ellingwood 2002). Performance-based design involves designing for a desired serviceability outcome rather than a strength requirement. For example, it may be desirable for a building to retain all its sheathing panels through the hurricanes it will experience in the next fifty years. Although it is possible to design a building for almost 100% reliability, such a task is often uneconomical. Therefore, much engineering design relies on probabilities. Studies known as "reliability analyses" aim to compare the probabilistic distributions for the applied load magnitudes and directions to the system component behavior in order to determine the probability a particular system will fail within a given time frame.

The integrity of the roof-to-top-plate connection has been identified as a key limit state for roof systems by many studies (Pinelli et al. 2004; Ellingwood et al. 2004; Rosowsky and Cheng 1999b). As such, it is essential that the load applied to this

connection be known. Currently, ASCE 7 provides a method for calculating wind loads as pressures that act on various zones of the building envelope. Little work has been done regarding tracking a load from its application on the sheathing down to the connections between the rafters and top plate.

System Behavior

The behavior of wood truss systems is very complex and influenced by load sharing, partially composite action of members and sheathing, and connection behavior (Rosowsky and Ellingwood 2002). Load sharing has been investigated by previous investigators. Sheathing has been shown to distribute load across the truss members, resulting in more load being absorbed by the stronger members (Criswell 1979). Subsequent studies have aimed to quantify the effects of load sharing via a load sharing factor for roof (Cramer, et al. 2000; Folz and Foschi 1989), floor (Folz and Foschi 1989) and wall (Rosowsky and Yu 2004) systems.

Other investigators have attempted to analyze the system behavior of wood truss assemblies directly, using structural analysis software (Mtenga et al. 1995; Gupta 2005). These studies suggest that system failure may not be controlled by the weakest component, and indicate that the roof system may need to be modeled as a parallel, rather than series, system if accurate failure probabilities are to be determined.

Past reliability analyses have considered only the statistical distributions pertaining to the capacity of individual components (Rosowsky and Cheng 1999b). Since the equivalent capacity of connections in a system is greater than the capacity of an

individual connection (Rosowsky et al. 1998), these analyses may not be accounting for the full strength of the system. Further investigation is necessary in order to understand the statistical distribution of system strength and its role in the reliability of the roof system as a whole. This research will consider system behavior effects in determining limit states, strength and load distributions in order to generate failure probabilities for low rise wood truss roof systems subject to high winds.

CHAPTER THREE

MODEL

Base Structure

Recent hurricane damages have devastated coastal communities and focused national attention on hurricane damage mitigation. The majority of existing structures in hurricane-prone regions are low-rise residential structures from the middle of the twentieth century (Rosowsky and Cheng 1999a). A representative structure was chosen as the basis for the model to increase the applicability of this study's results. The selected structure has a roof system that is believed to be typical of military base housing and coastal residences in hurricane-prone areas.

The model used in this study was based on an actual roof system found in the Douthit Hills apartment complex on the campus of Clemson University, shown in Figure 3.1. Past experimental work provided values for a variety of structural parameters used in model generation.



Figure 3.1: Douthit Hills structure (Shanmugam et al. 2009).

The roof frames for these buildings consisted of Southern Yellow Pine dimensional lumber. Trusses were spaced at 16 inches on center, and composed of 1.5" x 5.5" and 1.5" x 3.5" members as the ceiling joists and 1.5" x 5.5" elements as the rafters. These trusses were connected to the top-plate via a toe-nail connection of several long smooth shank 16-d common nails (Figure 3.2). Running parallel to the top-plate and serving as an additional load distribution path were 1.5" x 3.5" cross-members and 0.75" x 5.5" fascia elements. Solid 0.75" x 5.5" plank elements served as the roof sheathing and were covered in asphalt shingles.

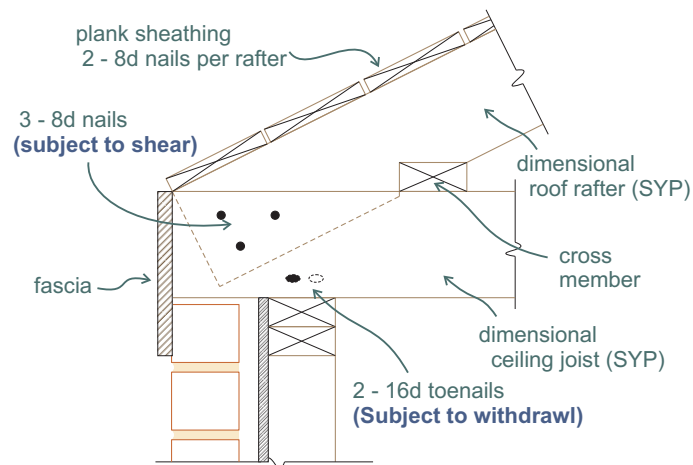


Figure 3.2: Detail of actual connection (Gleason et al. in review).

Modeling Medium

Design software packages, such as SAP2000 (Computers and Structures 2006) and ETABS (Computers and Structures 2005), are widely used by the structural engineering community. Assumptions about structural behavior are often built-in to these programs to

facilitate productivity in consulting firms. Limiting user control over more complicated parameters and using default settings allows engineers to obtain the approximate response of a structure under various scenarios. While designers can often use the programs' output with little adjustment, the resulting approximations from many design program analyses are often not appropriate for analytical research work.

One of the main drawbacks of these commercial packages is their limited nonlinear analysis capabilities. Nonlinear behavior has been observed in wood roof systems, particularly in the roof-to-wall connection. Appropriate modeling of the load redistribution path requires this nonlinear behavior to be addressed. OpenSees (McKenna 2009) , a software framework for structural and geotechnical applications created by researchers at the University of California, Berkeley, was chosen as the modeling medium for this study because of its superior nonlinear analysis capabilities. Additionally, previous work (Shanmugam et al. 2009) generated a nonlinear model of the roof-to-wall connection in Opensees; using this framework eliminated compatibility issues or having to redevelop the model.

Structural Model

The model was generated with consideration given to system effects, computation time, wind pressure distribution and previous investigation of the behavior of the actual structure. This study uses a model consisting of 12 trusses taken from the end of the roof (Figure 3.3). It is well-known that structures consisting of repetitive members have a higher load capacity than the sum of individual components due to system effects

(Cramer et al. 2000). The consequences of this on load distribution and redistribution are captured by using a system of twelve trusses. Adding more trusses would give some additional information, but significantly increase the required computation time and limit the number and variety of simulations that could be run. Locating these trusses near the end of a building provides sufficient information about the structure's response under both interior and end zone wind pressures, while keeping computation and modeling time reasonable.

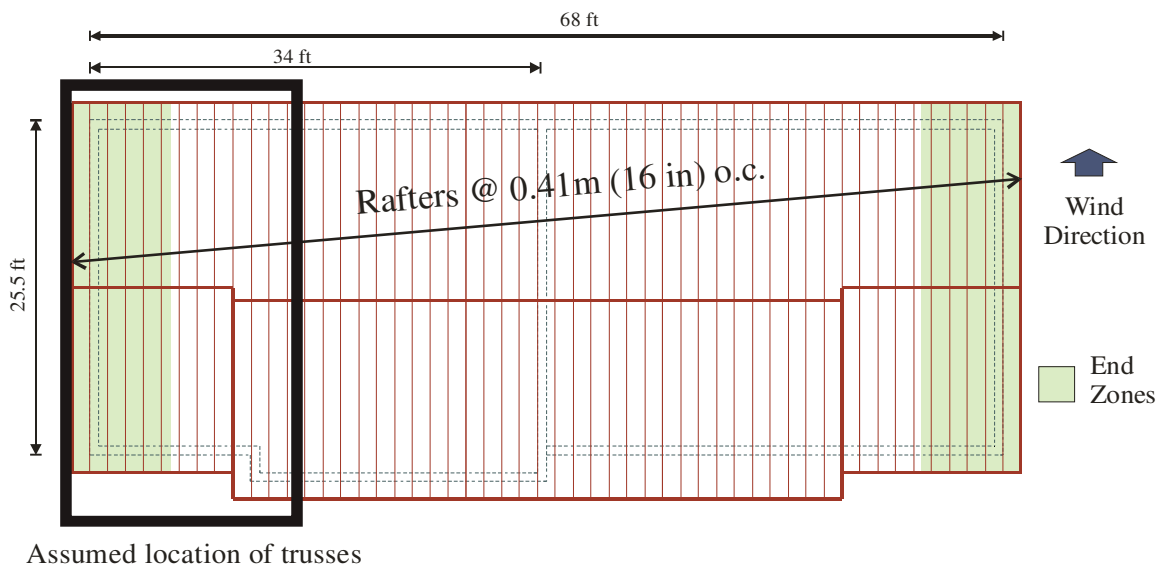


Figure 3.3: Assumed location of trusses in this study (adapted from (Shanmugam et al. 2008)).

A rendering of the model is shown in Figure 3.4. Each truss spans 362 inches and consists of one 2x6 ceiling joist and two 2x6 has rafters, which slope at 22 degrees. Cross members and fascia elements, as in the original structure, connect all trusses and are modeled as a beam element with combined properties. To simplify the modeling task

beam-column elements were used instead of shell elements to model the sheathing planks.

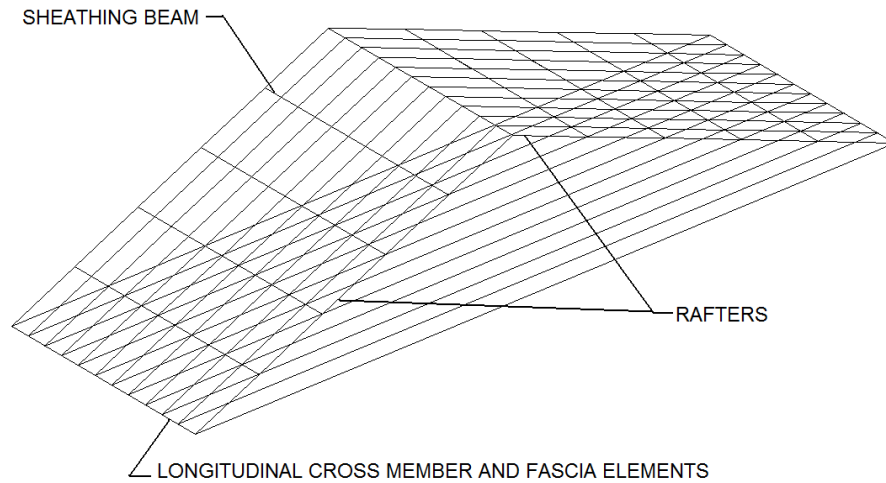


Figure 3.4: Rendering of model.

Two sheathing beams exist at the fifth-points along each rafter. Each beam has the aggregate properties of the 3.5 sheathing planks falling within its tributary area. This concept is illustrated in Figure 3.5. It was assumed that the actual overlapping configuration of sheathing panels results in longitudinal moment transfer between end-to-end panels, but restricts moment transfer in the transverse (side-to-side) direction. Accordingly, the longitudinal strips of panels were modeled as continuous beam-column elements. These elements were attached to the rafters at each joint, and no constraints were placed on the relative rotation between adjacent beam-column elements in the transverse direction.

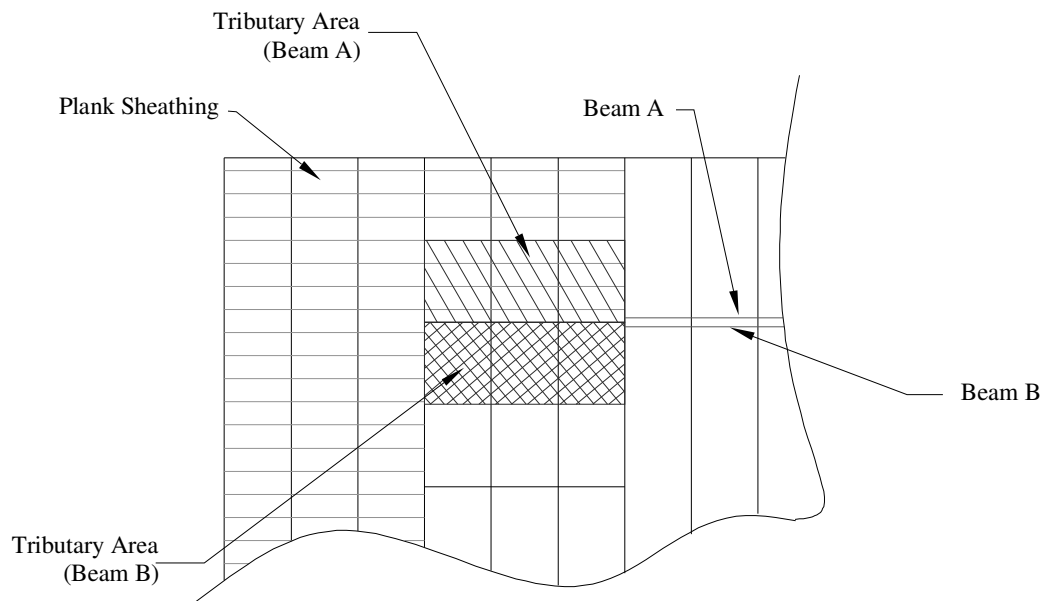


Figure 3.5: Assignment of tributary properties to sheathing beams.

Structural parameters for the sheathing and truss elements were taken as linear elastic deterministic values. The design values published in the NDS Supplement (American Forest & Paper Association, Inc. 1993) provided substantial accuracy for this study, and the modulus of elasticity was taken to be 1700 ksi. Past research has proven that the system failure is not dramatically influenced by these material properties. System failure is a result of a break in the uplift load path. Post-hurricane damage reports have shown that the roof-to-wall connection, not the individual elements, is critical (van de Lindt et al. 2007).

Roof-to-wall Connection Model

The system is supported at two discrete locations (Figure 3.6) on each truss. The end points are supported by a tension only spring model for a typical roof-to-wall connection, developed in a past study (Shanmugam et al. 2009). Previous reliability analyses have not accounted for the true behavior of the roof-to-wall connection, and used either a constant value for the connection capacity or a limited probability distribution of uplift capacity values (Rosowsky and Cheng 1999a; Cheng 2004). This may be an inaccurate assessment of the toenail connection's behavior. The current study aims to ascertain the error induced by such assumptions in estimating the probability of and manner in which system failure occurs.

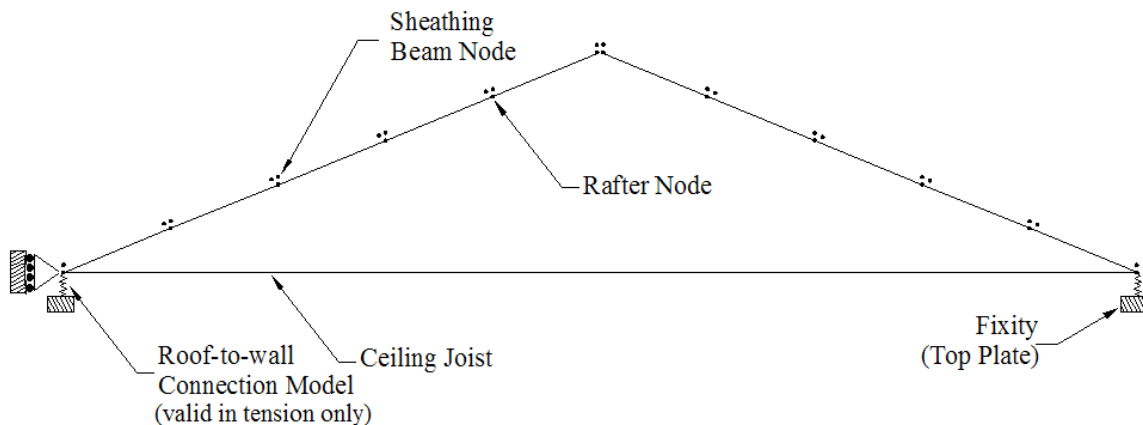


Figure 3.6: Truss model.

The response behavior of an in-situ toe-nailed connection is quite complex. Under a gravity load, the top-plate bears the load, and the support is essentially rigid. When

subjected to uplift, field tests have revealed the nonlinear behavior of these connections (Shanmugam et al. 2009). The previously developed (Shanmugam et al. 2009) OpenSees connection model idealizes this as multi-linear behavior governed by three primary parameters: ultimate uplift capacity (F_{ult}), initial stiffness (k_0) and displacement at peak load (u_2).

Figure 3.7 shows the generalized force-displacement behavior of the connection model. As load is applied, the connection exhibits a linear response with an initial stiffness of k_0 . When the load reaches some limiting force, s_1 in Figure 3.7, the behavior remains linear, but is governed by a different stiffness value. Once the connection's peak capacity, F_{ult} , has been reached, load is gradually shed, until a displacement of u_3 . This idealized behavior has been proven appropriate by comparing the amount of energy dissipated in a model connection to experimental results from actual connections (Shanmugam et al. 2009).

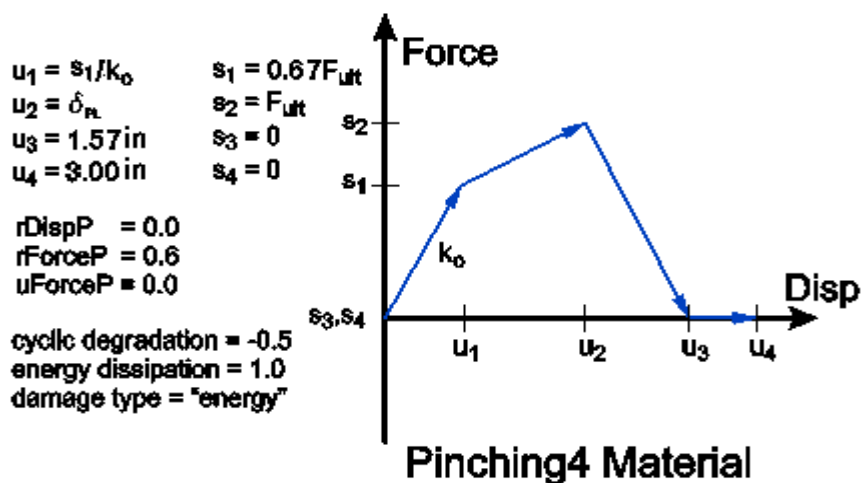


Figure 3.7: Force-displacement behavior of analytical connection model (adapted from Shanmugam et al. 2009).

Due to variability in construction techniques, the connection behavior can be very different over all locations in a roof structure. Based on previous in-situ tests, probability distributions and correlation coefficients have been generated for each of the governing behavioral parameters: F_{ult} , k_o and u_2 . A lognormal distribution is assumed for the capacity (F_{ult}) based on in-situ tests carried out in a previous study (Shanmugam et al. 2009). Two-nail toenail connections, with parameters shown in Table 3.1, are assumed for this study. Experimental results show that initial stiffness is best characterized by a normal distribution, and displacement at peak load is only plausibly described by a 3-parameter Weibull distribution.

2-16d toenailed connection	Uplift Capacity (F_{ult})		
	lbs		
	Distribution	l	z
	lognormal	5787	0.34
	Initial Stiffness (k_o)		
	lbs/in		
	Distribution	m	s
	normal	2126	768
	Displacement at Peak Load (u_3)		
in			
Distribution	k	u	e
*weibull	1.299	0.336	0.13

* k = shape factor, u = scale factor, e = threshold

Table 3.1: Probability distributions for analytical connection model (Shanmugam et al. 2009).

The correlation between these parameters must be addressed in order to obtain a realistic distribution of connection capacities. Significant correlation (correlation coefficient, $\rho = 0.62$) exists between uplift capacity and stiffness, while correlation

between other parameters was lower (initial stiffness and displacement at ultimate load: $\rho = 0.096$, ultimate capacity and displacement at ultimate load: $\rho = 0.393$). These distributions were utilized in the Monte Carlo simulation to incorporate the uncertainty in connection behavior observed within a given structure.

Load Distribution

The failure of the system is based on the amount of load carried by each component relative to its capacity. For the given roof system, load is applied to the sheathing elements, and transferred through the structure to the roof-to-wall connections, which function as supports for the model. An accurate representation of the load path within the structure is, therefore, essential.

The primary method of distributing the load from its point of application to the roof-to-wall connections is the sheathing. Wind pressure loads are applied to areas of sheathing panels, which transfer the load to the truss rafters. Recall that the sheathing beams are able to transfer moment longitudinally over rafters, but not in the transverse direction.

Since the sheathing elements are relatively rigid compared to the rest of the structure, load is distributed to the rafters by relative stiffness. The relative stiffness of rafter elements is a function of the connection behavior at the roof-top plate joint. This fact highlights the need to consider connection stiffness and behavior variability when analyzing the roof system, which has not been considered in past reliability studies.

To effectively capture the nonlinear behavior of the connections, load is applied incrementally. When individual connections are pushed past their initial linear regions, their stiffness decreases, and they carry a lower proportion of the incremental load. While the capability of the connection model to capture this change in behavior is important, its key advantage over previous models is the ability to gradually shed load when loaded beyond its uplift capacity.

As a failed connection continues to displace, its load is redistributed through the sheathing, cross-member and fascia elements to the remaining connections. Past studies operated under the assumption that this additional load would proceed to overload all remaining connections; this failure mode is commonly referred to as a “zipper effect” (Shanmugan, B. 2008). Though this might be a valid assumption if all connections had identical behavioral properties, the inherent material variability of wood and differences in construction techniques, amongst other factors, all contribute to the diversity of roof-to-wall connection behaviors observed in a structure. Previous research has suggested that ultimate capacity and initial connection stiffness both have coefficients of variation (COV_5) of 0.36 (Shanmugam et al. 2009).

Model Verification

The integrity of any analytical analysis is a function of the model’s ability to adequately capture the actual structure’s behavior. Several nuances of the model were further investigated prior to full analysis to ensure appropriate behavior. This section discusses these experiments.

Sheathing Sensitivity Test

After preliminary tests, loads appeared to be distributed too evenly across the connections. Overly stiff sheathing elements were suspected to be the cause; if the relative stiffness of the sheathing was too high, it would act as a rigid shell and all connections would deform equally. Since all connections for this test had equal stiffness, the result would be approximately equal reactions at all nodes.

To check this assumption, sensitivity analyses were run for the same twelve truss structure with identical behaviors for all roof-to-wall connections and a uniform vertical load applied to the entire system. Values of I , $I/100$ and $100*I$ were used in determining the sheathing beams' moment of inertia, with I being the calculated value of the moment of inertia – $I_y=445.83\text{in}^4$ for a 0.75" x 5.5" plank. Analyses were run both with and without the fascia and cross-members as distribution elements to determine the primary load distribution path.

All load was eventually transferred through the structure to the twenty-four support nodes, at the base of the roof-to-wall connection. This location corresponds with the top-plate in the actual structure, which was assumed relatively rigid for this study. Figure 3.8 shows the relative distribution of load to one such support node. For all six cases of sheathing stiffness, a typical interior connection takes between 4.0% and 4.5% of the load, if applied uniformly. Although the percentage of load carried by a given node is not independent of the effective stiffness of the distribution elements, the influence of stiffness variation is minimal in the range considered.

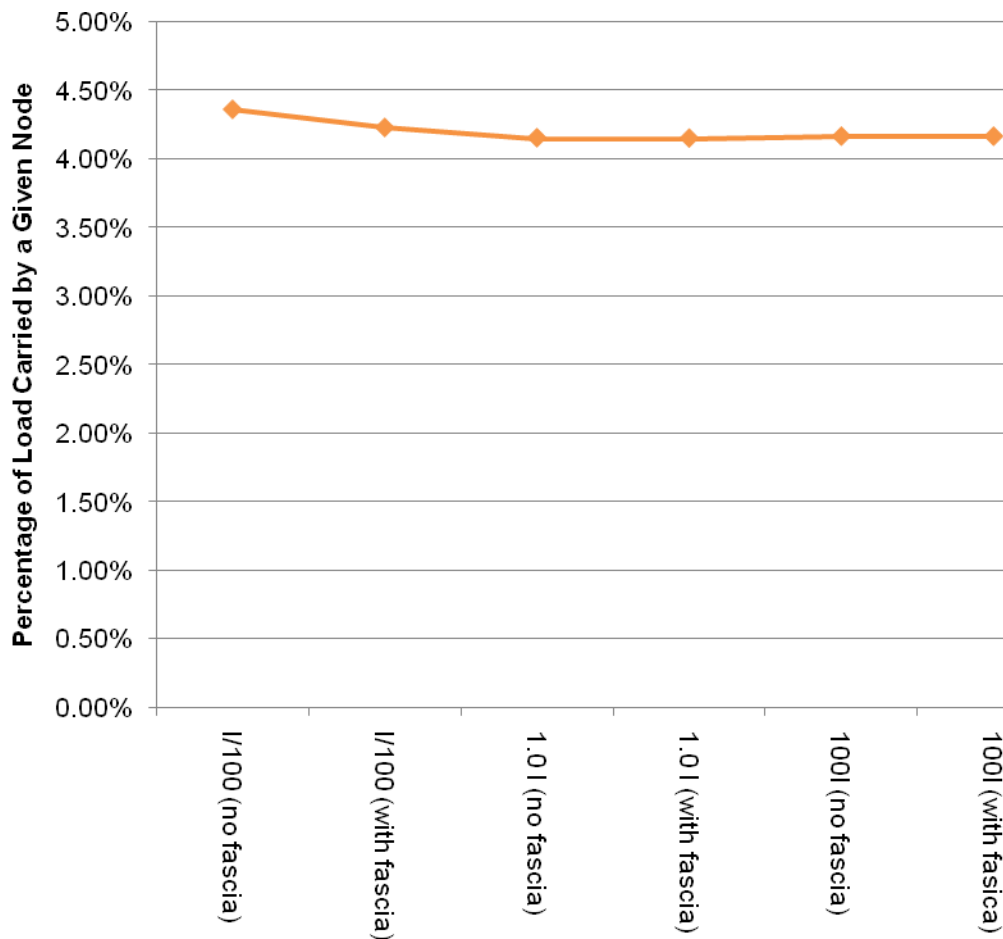


Figure 3.8: Effect of sheathing stiffness on load distribution.

Failure Sequence

One of the primary goals of this research was to determine how many connections needed to fail before a system failure would ensue. Structural analysis suggests that only three connections are required for the truss to remain stable, yet past reliability studies have assumed that the system fails after only one connection exceeds ultimate capacity (Shamugam, Nielson and Gleason 2008). Sometimes called the “zipper effect”, these

studies refer to the idea of a series system failure. The redistribution of the failed connection's load is assumed to cause all other connections to fail in turn, rendering the structure unstable.

Limited work has been done to determine appropriate limit states as well as assumptions regarding the roof system behavior (Shamugam, Nielson and Gleason 2008). A simulation-based approach was used in conjunction with a model to determine the fragility of the system utilizing two different limit state assumptions. First, the limit state was taken to be the failure of any single connection, assuming a series system failure. These results were compared to those found when system failure was defined by the failure of four adjacent connections, with load redistribution after the failure of any single connection. Statistical values for uplift capacities for the roof-to-wall connections were determined experimentally on full-size existing structures. Probabilistic models for wind and dead loads were based on models from previous work (Rosowsky and Cheng, 1999).

Results from the Shanmugam et al. (2008) study showed that assuming a series system failure greatly overestimates the fragility of the system. As seen in Figure 3.9, for a wind speed of 120mph and exposure category C, the probability of a series failure is 60% while the probability of failure for four adjacent connections is only 30%. All other wind speeds and exposures followed this general trend. The study recommended that conditional probabilities for failure of one connection given failure of others be used in subsequent reliability studies.

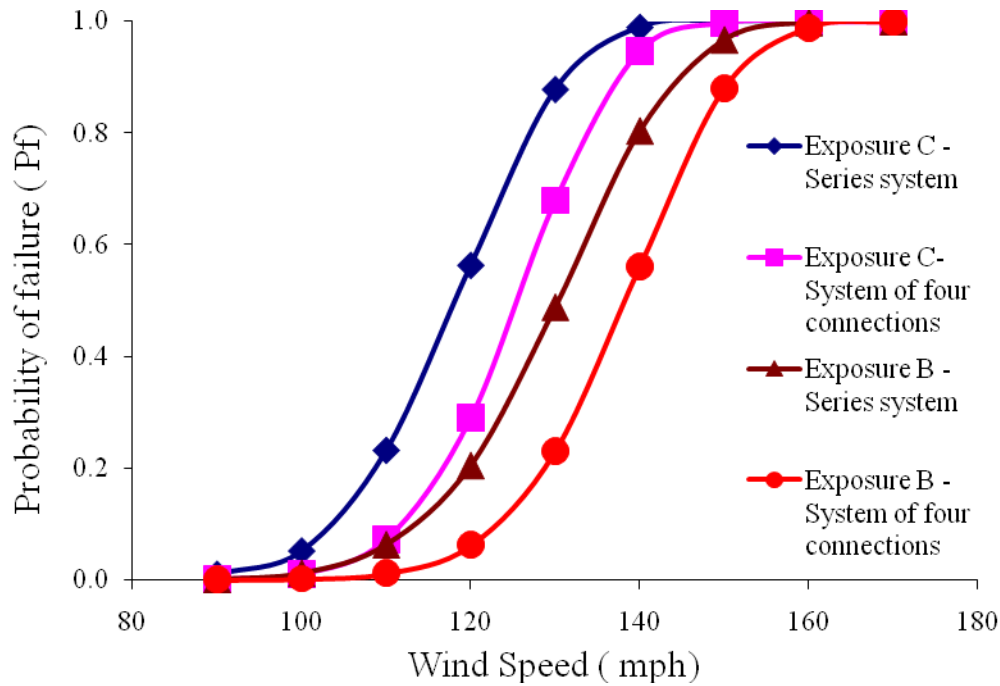


Figure 3.9: System fragility curves for different exposure categories (adapted from (Shamugam, Nielson and Gleason 2008)).

Preliminary simulation results from the current study neither confirmed nor refuted this concept. The failure sequence seen in preliminary simulation was puzzling and somewhat inconclusive. Often, the model would fail with only a few of its connections nearing capacity. Further investigation was conducted to determine if this was because the subsequent load step would push all connections beyond their capacities or if the model was flawed.

Since the sheathing acts as a diaphragm, load is distributed to the individual roof-to-wall connections according to their relative stiffness. When all connections have the same stiffness, load is distributed according to tributary area. Under a uniform load, the outermost roof-to-wall connections in this scenario will carry the least load due to their

smaller tributary areas. Only half of the actual tributary area was considered for the connections on the truss nearest the rest of the structure (Figure 3.3), which was not modeled. Consequently, if all connections have the same ultimate capacity, the outermost connections should fail last. The ultimate capacity, F_{ult} (see Figure 3.7), of these connections was manipulated to surpass the capacity of the interior connections, but maintain the same stiffness as to attract an identical proportion of the applied load. Eventually, the interior connections would fail, and all of the applied load would be redistributed to the exterior connections. As the structure was loaded, failure began at the central connections and propagated outward, as shown in Figure 3.10. Scenarios with various configurations of higher strength corner connections were checked. In all cases, the loading, off-loading and redistribution followed what was expected, validating the model.

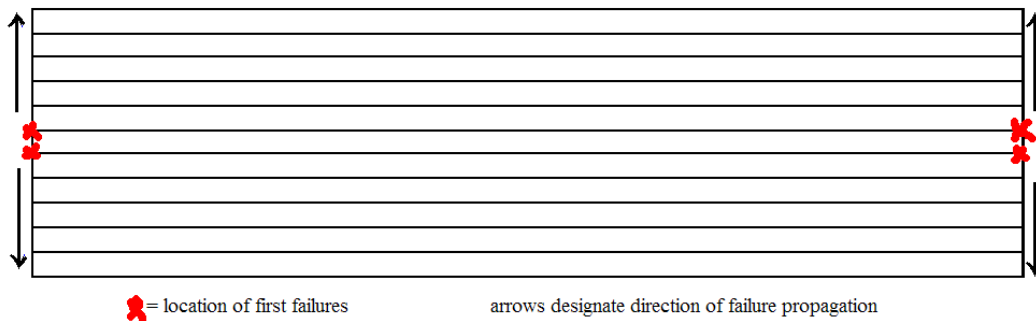


Figure 3.10: Connection failure propagation under uniform load.

It was determined that the reason simulated models did not behave accordingly was the small range of connection values. In order for the four exterior connections to have sufficient capability to absorb the other 20 connections' load, their F_{ult} value must be over

100 times greater than that of the interior connections. This is unrealistic as the probability distribution for this value has a zeta value of only 0.34, with a median value of 326 lbs.

Therefore, the load step was too high to sufficiently see the individual failure of each given connection given such a large difference in connection capacities. Somewhat of a “zipper effect” does exist, just not the extent seen in the preliminary results; a single failure is not necessarily equal to a system failure. This idea is explored further in the actual simulations, discussed in Chapter Five.

CHAPTER FOUR

WIND LOADS

As a fluid, the dynamic behavior of wind (air) is quite complex. Its velocity is highly influenced by surrounding obstructions, ground conditions and temperature. The pressure felt by a building is proportional to the square of velocity. Due to velocity variations, the resulting wind pressure on a building is neither static nor uniform. Structures are often analyzed as if wind loads are ideal because of the complications involved in capturing a true wind load. This chapter discusses assumptions regarding the behavior of wind, describes the methods used for determining wind loads, and explains the generation and application of wind loads used in this study.

Wind Behavior

The behavior of wind is variable with respect to both time and space. In spite of the abundant research investigating fluid dynamics, definite relationships and behavioral constraints for wind speeds and pressures are limited. This is because wind is neither slow enough nor viscous enough to utilize simple fluid mechanics equations, which were derived for laminar flow (Cook 1985). Laminar flow is the state in which a fluid's motion can be described as steady, and is governed by the viscous shear stresses of layers of fluid sliding past one another. Instead, the behavior of wind is unsteady and highly variable, a characteristic of turbulent flow (Cook 1985).

Turbulence is the chaotic and random fluctuations observed within a fluid's motion. These fluctuations are a result of applied stress. For wind, this applied stress can come in several forms. As wind passes over terrain, the ground essentially applies a frictional force to the lowest layers of wind. If wind had either a higher speed or viscosity, the lowest layer would simply slow down due to this drag force, resulting in a varying velocity distribution with respect to distance about the ground, as shown in Figure 4.1 (a). Due to wind's speed and low viscosity, the surface roughness results in an unsteady, turbulent boundary layer, shown in Figure 4.1 (b).

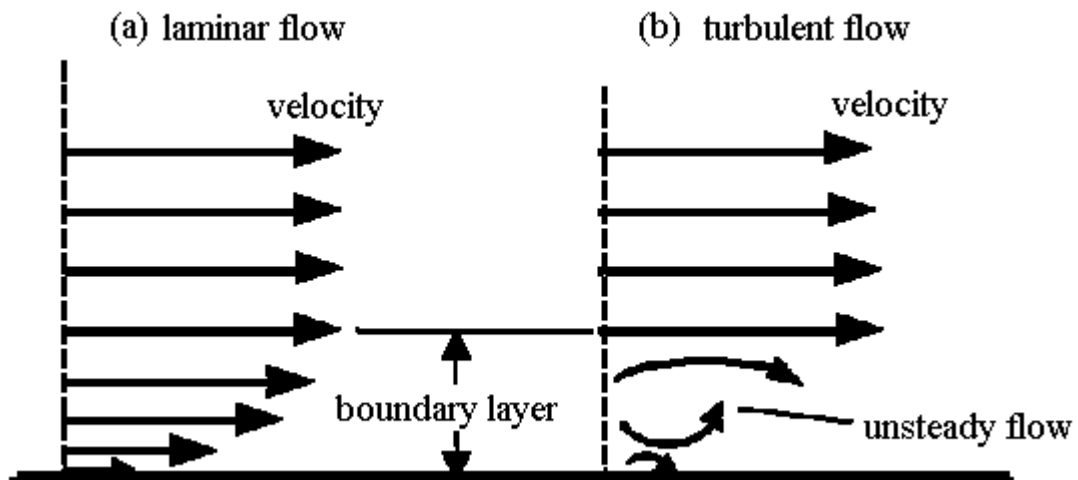


Figure 4.1: Velocity profiles and boundary layers for laminar and turbulent flows (adapted from NASA).

Obstructions within the flow path also affect wind velocity. Topographic features, such as valleys and hills, as well as neighboring structures or trees can all be classified as obstructions with respect to wind flow. When faced with an object in its path, the

effective flow area of the wind is reduced, which results in an acceleration. These obstacles can also cause local fluctuations resulting from separation bubbles. Having to abruptly change direction results in localized eddies and vortices, as shown in Figure 4.2.

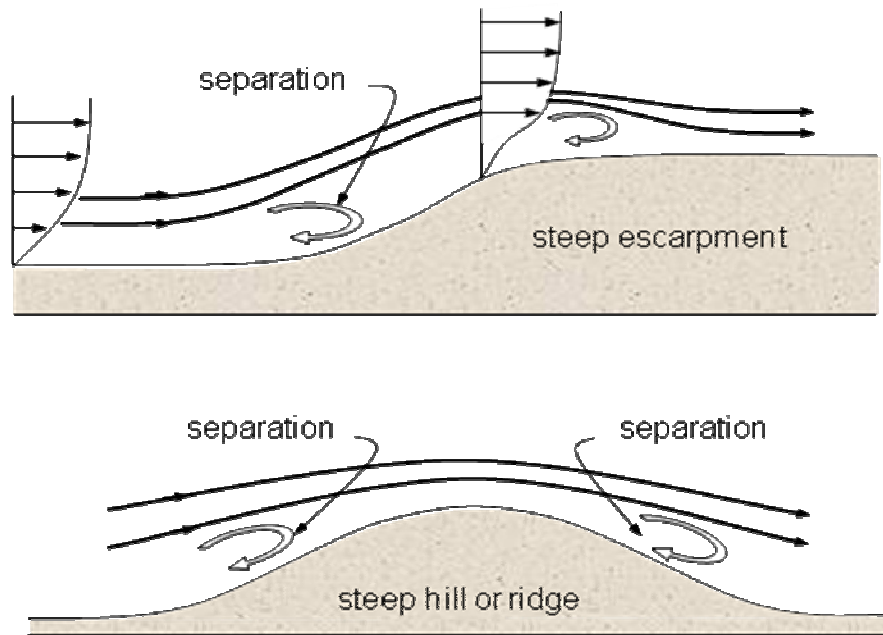


Figure 4.2: Effect of obstructions on wind velocity (Holmes 2001).

Wind Loads

As wind passes around a structure, it exerts a pressure on the building. The magnitude of this pressure is taken to be proportional to the square of the velocity. Though seemingly simple, the calculation of roof wind pressures is made difficult by the variable wind speeds over and around the structure. Local fluctuations, structural obstructions, the temporal variation in the base wind speed and direction are all factors

that influence the wind speed at a given location. These variations in wind speed, in turn, complicate the calculation of wind pressures.

Despite wind's fluctuating and turbulent nature, a region's horizontal wind speed can be treated as statistically stationary for the purpose of ascertaining structural loads. The atmospheric boundary layer and weather systems that produce strong winds are two of the primary influences on wind speed (Cook 1985). Low-rise buildings have such a small height ratio with the boundary layer that they can be considered independent of its effects (Cook 1985). Weather system effects are akin to ambient wind turbulence, which varies with time. Depending on the averaging period, this atmospheric turbulence may be negligible. A frequency domain plot of the horizontal wind speed developed by van der Hoven (1958) is shown in Figure 4.3. This plot shows that, for periods of ten minutes to two hours, wind's statistical parameters remain constant. Since wind load durations for analysis fall in this time range, utilizing a single set of statistical parameters can be used to reasonably approximate the wind velocity at any given point in time.

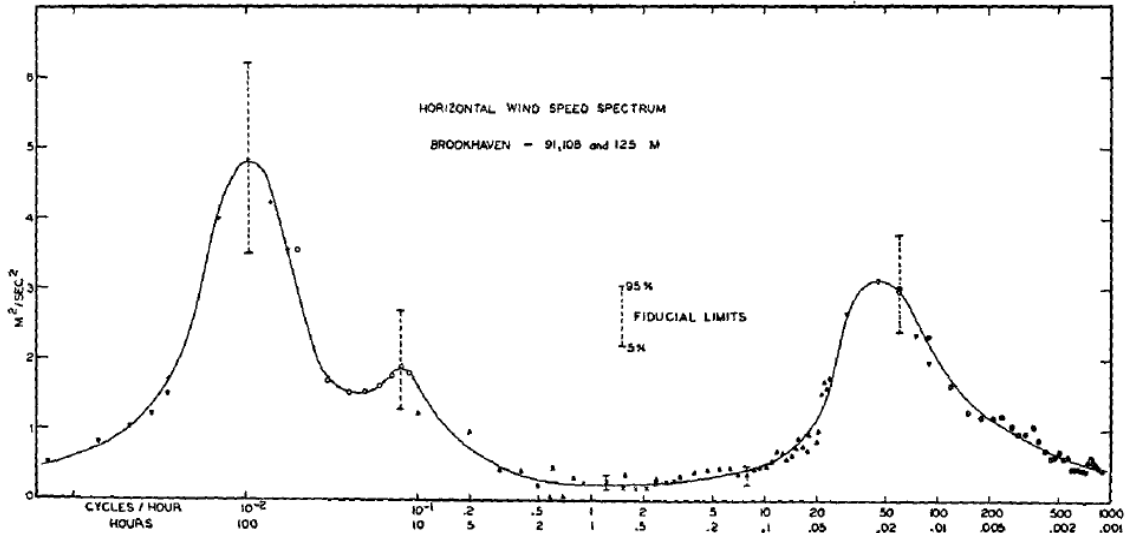


Figure 4.3: Spectrum of horizontal wind speed (van der Hoven 1958).

While temporal variations may not require consideration, spatial variations in wind speed cannot be neglected. In addition to the effects of terrain and topography, the structure itself has a significant influence on its own wind loads. For LRWF roof structures, the roof geometry is the dominating factor. Typically, low slope roofs will have negative pressure acting over the entire roof, regardless of wind direction. Roofs with a steeper slope will have positive pressures acting over the windward side, and suction pressures on the leeward side. This difference is due to the wind's inability to abruptly shift direction as it passes over the ridge. Additionally, closer to the end of a building, wind pressures will be higher, as there is less roof sheathing ahead of them to slow down the velocity. Figure 4.4 illustrates this concept.

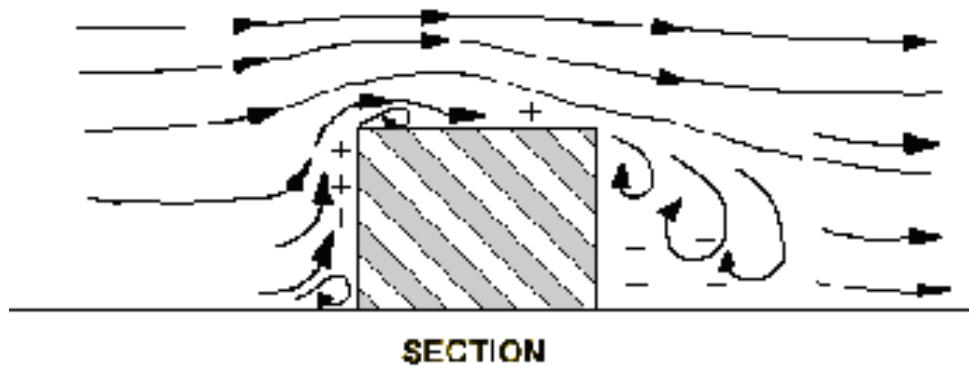


Figure 4.4: Wind flow around a structure (Hunt 2005).

Modeling Methods

A method of modeling wind loads is required for both research and design. There are currently two main schools of thought on wind modeling: the simple approach and the complex approach.

Simplified Approach

The simplified approach is similar to that used in design codes. This method assumes that the pressure is static and constant over a large area of the roof. Variations in the load with respect to time are not considered, and only macroscopic spatial differences are addressed. Several research studies (Ellingwood et al. 2004; Rosowsky and Cheng 1999a) have used a modified version of the procedure outlined in ASCE 7: Minimum Design Loads for Buildings and Other Structures (ASCE 2005). In this approach, wind pressure, q_h , is calculated by equation (1) which is a slight variation of Eqn 6-15 in ASCE 7 (2005):

$$q_h = 0.00256 K_h K_{zt} K_d V^2 \quad (4.1)$$

where K_h is the exposure factor, K_{zt} the topographic factor, K_d the directionality factor and V the 3-s wind speed at a height of 33ft. These factors account for differences in the mean roof height, surrounding topographic conditions and variability of the wind direction.

This base pressure is then modified by a coefficient, particular to the region of the building envelope where the pressure is to be applied. Figure 4.5 shows the ASCE 7-specified zones. In research, unlike design, statistical parameters for the distribution of these variables and zone coefficients are often used to address the uncertainty of the wind and building characteristics (Ellingwood et al. 2004; Lee and Rosowsky 2005; Rosowsky and Cheng 1999a).

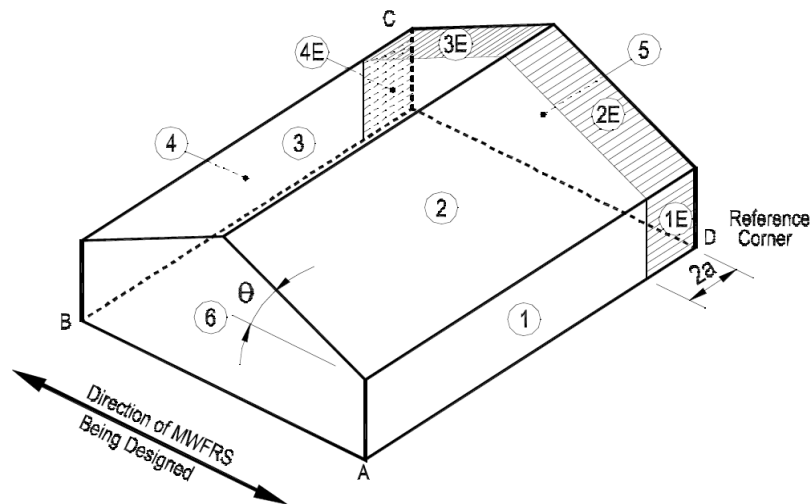


Figure 4.5: Wind zones used for method 2 calculations (ASCE 7-05).

The rigidity of the building is often sufficient to neglect the dynamic load effects, but not spatial variations. Based on building geometry, vortices may form near sharp corners and edges. These local turbulence effects cause significant pressure differences over a small area. Although spatial variations often average out to zero over a large area, they have large impacts on small areas, necessitating consideration of these variations in determining forces internal to the structure. ASCE 7 recognizes this by requiring additional load for components and cladding, with the pressure calculated based on the element's tributary area, called the effective wind area in ASCE 7 (ASCE 2005). Still, there are shortcomings to the use of this method for analysis. The roof is broken into discrete zones (Figure 4.6). These zones are a minimum of 9 ft² and capped only by the dimensions of the building (ASCE 2005). It is highly possible that the zones are too large to capture local fluctuations, which affect the load distribution throughout the structure.

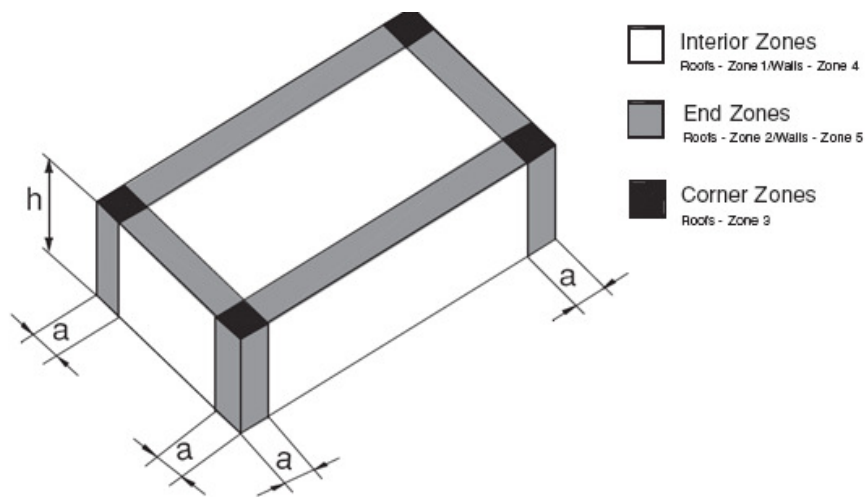


Figure 4.6: Components and cladding wind zones (adapted from ASCE 7-05).

Complex Approach

The complex approach aims to address many of the variables surrounding wind loads. One example of this approach would begin by collecting a very large amount of time histories for an infinite number of points along the roof, finding their stochastic parameters, and then generating correlations between the pressures over the entire roof. Simulations would then be run, with different wind speeds and structural capacities selected for each realization. This type of treatment for modeling wind loads is desirable, yet still appears to be impractical. Simulation approaches require running many different wind scenarios ($\sim 1 \times 10^4$). When using full wind time-histories the computational cost becomes excessive. This greatly limits the practicality of performing parametric studies. Therefore, a compromise between the simplified and complex approaches is sought.

Modeling Approach

This study uses a hybrid of the two theories, and aims to utilize the simplicity of calculating wind pressures via the ASCE 7-05 method while accounting for local pressure fluctuations that may impact the load distribution and, ultimately, the response of the structural system.

Pressure Data

Several different wind loads were evaluated for this study. Wind speeds of 100 mph and 130 mph for a direction of $\theta = 90^\circ$ (see Figure 4.10) in exposure category C were used for this study. These conditions were chosen to correspond with typical hurricane-prone regions, while providing some basis for comparison between the probabilities of

failure for wind speeds. Several statistical distributions have been proposed for wind loads, including lognormal (Ellingwood and Tekie 1999), extreme value type I (Endo et al. 2006), extreme value type III (Endo et al. 2006) and gamma (Tieleman et al. 2007) distributions. This study assumes a lognormal distribution.

Statistical parameters for each of these wind loadings were calculated using previously developed procedures. Base pressures were calculated per Method 2 of ASCE 7-05 (ASCE 2005), using the standard directionality factor of 0.85, a topographic factor of 1.0, and ignoring the importance factor. These code based values were then reduced fifty-nine percent to determine the median pressures, in accordance with work done by Rosowsky and Cheng (1999a 1999b). Probability model values for each zone are shown in Table 4.1, with $\lambda = \ln(\text{median value})$ and coefficients of variation represented by ζ .

Table 4.1: Wind load distribution parameters.

Zone*	V= 100mph		V=130mph	
	λ [psf]	ζ	λ [psf]	ζ
2	2.24	0.41	2.77	0.41
3	2.02	0.41	2.55	0.41
2E	2.51	0.41	3.03	0.41
3E	2.15	0.41	2.68	0.41

* see Figure 4.5

The trusses used in this study are located on the end of the structure (Figure 3.3), and fall in zones 2, 2E, 3 and 3E for a transverse wind (Figure 4.5). Within each of the four ASCE 7-05 zones, the roof is broken up further into discrete sub-regions to account for local fluctuations (Figures 4.7). Each sub-region is 39.11" x 16", smaller than a typical

sheathing panel. This size was determined by dividing each rafter into five sub-members and creating areas spanning the sixteen inches between trusses. Generation of wind pressure realizations for each panel requires information about wind pressure marginal probability distributions (Table 4.1) and the spatial correlation between these distributions. Wind pressure realizations were performed in MATLAB (MathWorks). Figures 4.8 and 4.9 show the median wind pressures assigned to the various sub-regions.

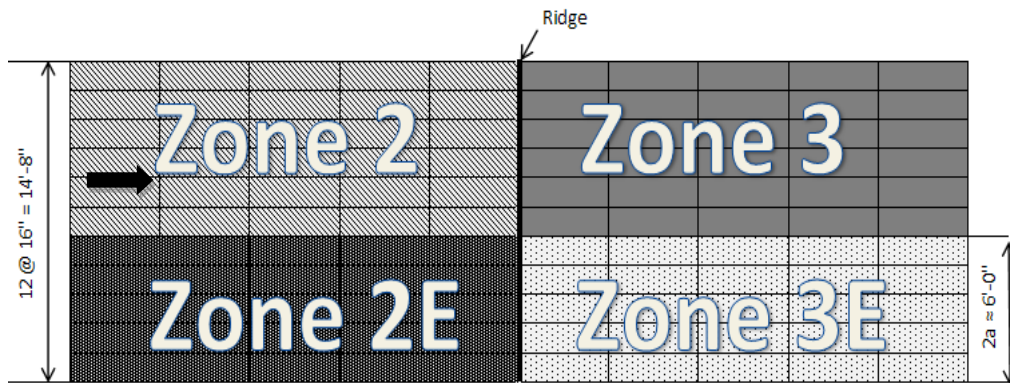


Figure 4.7: Sub-region locations.

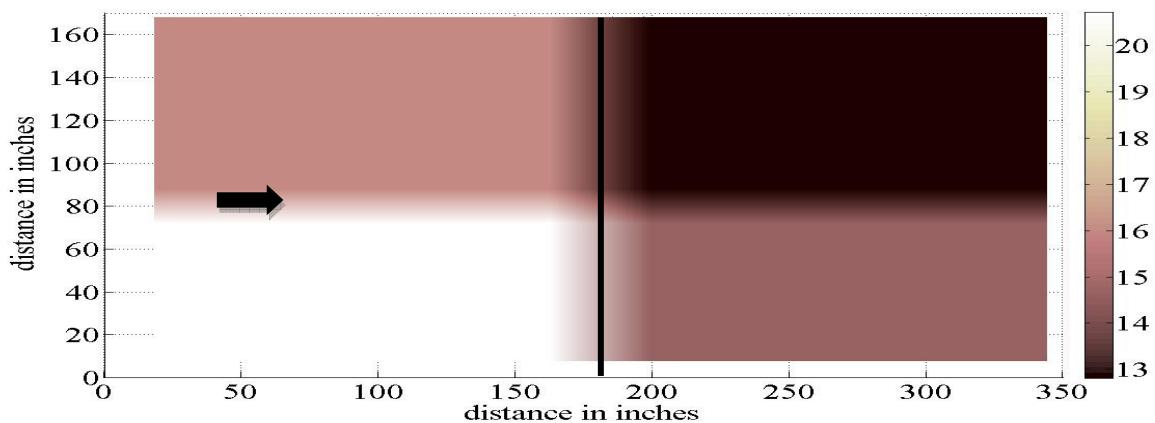


Figure 4.8: Median wind pressures (in psf) for 100 mph wind speed.

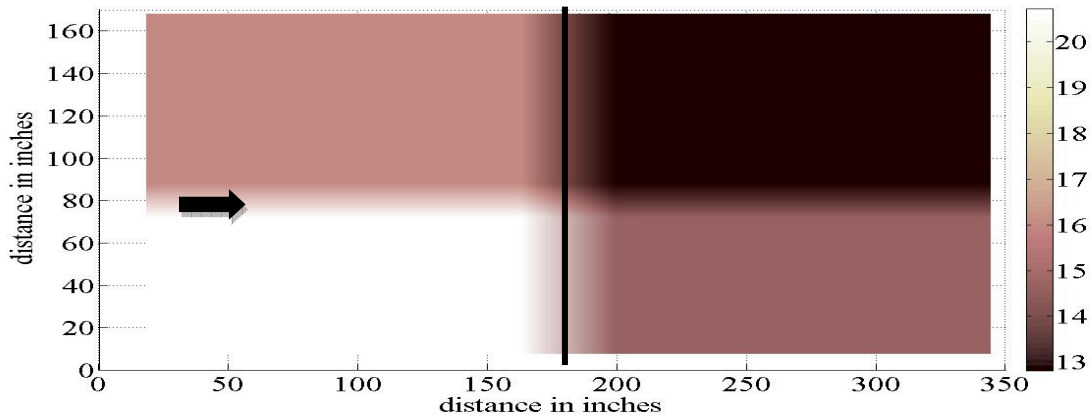


Figure 4.9: Figure 4.9: Median wind pressures (in psf) for 130mph.

Correlation Coefficients

Accounting for the correlation between various pressures over the roof is imperative. While pressures are randomly generated, constraints are necessary to ensure these random values are realistic. The best method for ascertaining these constraints would be to experimentally determine the correlation between wind pressures at many points across the roof system as a function of the distance between them.

As a preliminary approximation, wind tunnel data from the windPRESSURE program was utilized (Main 2006). This data was based on measurements collected at the University of Western Ontario's wind tunnel. Hundreds of pressure taps were placed on a model building with a roof slope of 22° and length scaling of 1/100. Tests were run for a single wind speed at various directions in surface roughness conditions similar to open country terrain, and pressure data was collected at a frequency of 500Hz. The resulting data is stored in a database accessed via the software program windPRESSURE (Main 2006), and intended to be scaled with building dimensions for a variety of structures.

Correlation coefficients for this study were derived from the data in this database, compiled by researchers at Michigan Technological University (Yin 2009)

A single correlation matrix was developed for use in this study based on pressures for a wind speed of 100mph at an angle of $\theta=75^\circ$ (Figure 4.10). It was assumed that the correlation between pressures was not significantly affected by wind speed. Correlation for winds acting at $\theta=75^\circ$ was assumed to be similar enough to that for wind travelling perpendicular the ridge ($\theta=90^\circ$), as this data was not available from the windPRESSURE database. Again, it is expected that future work will refine this method and data to improve accuracy.

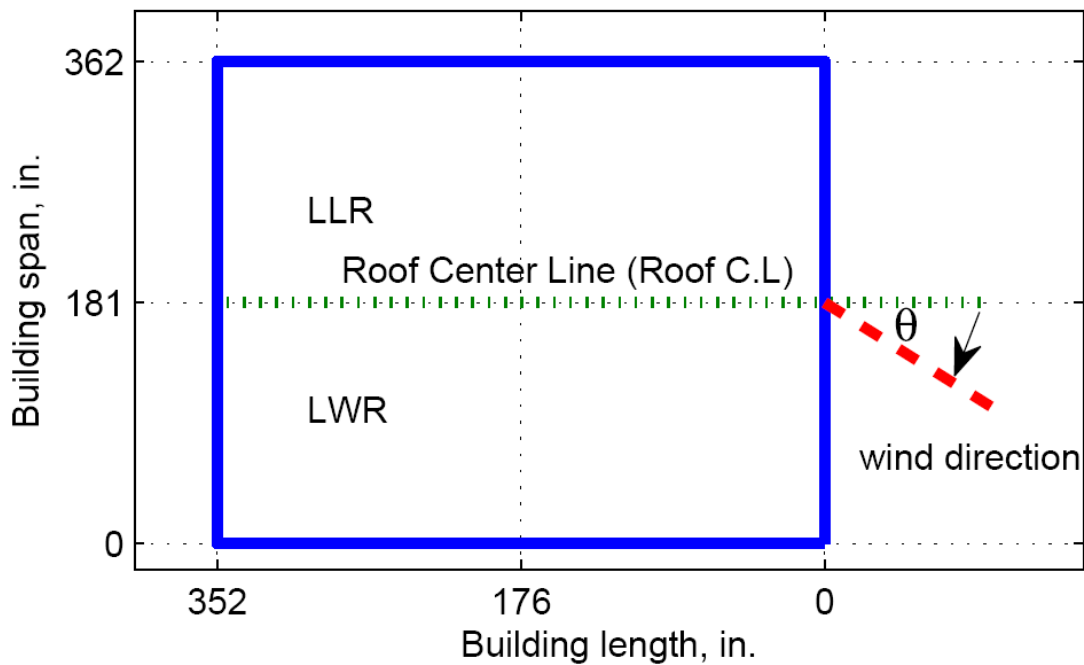


Figure 4.10: Top view of wind direction (Yin 2009).

A time series of pressure coefficients at various taps in specified grid-like locations (Figure 4.11) were generated for the model structure, which was described in Chapter 3. The correlation of pressure data at a single time step and distance between points was determined and plotted (Figure 4.12). A cubic equation was shown to be a reasonable representation of the correlation. This equation was used to develop the correlation matrix for the each of the sub-regions' wind pressures, where d is the distance between any two sub-regions.

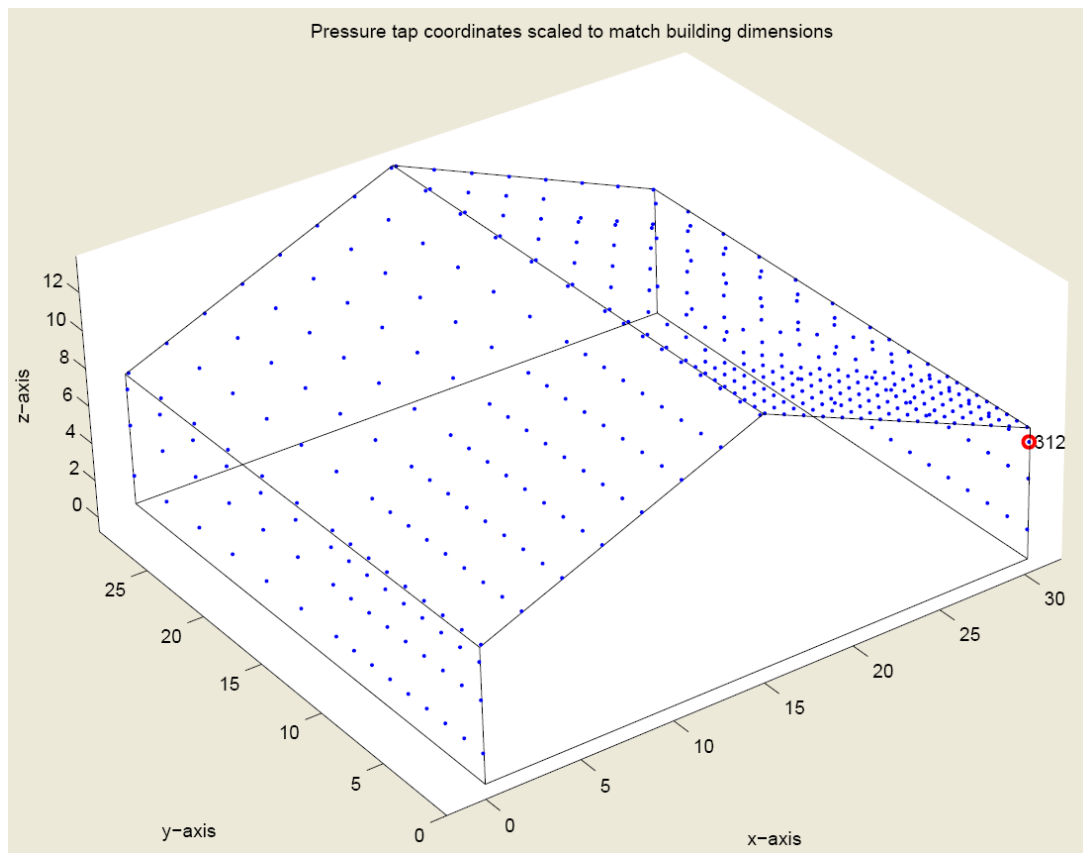


Figure 4.11: Building model with taps by windPRESSURE (Yin 2009).

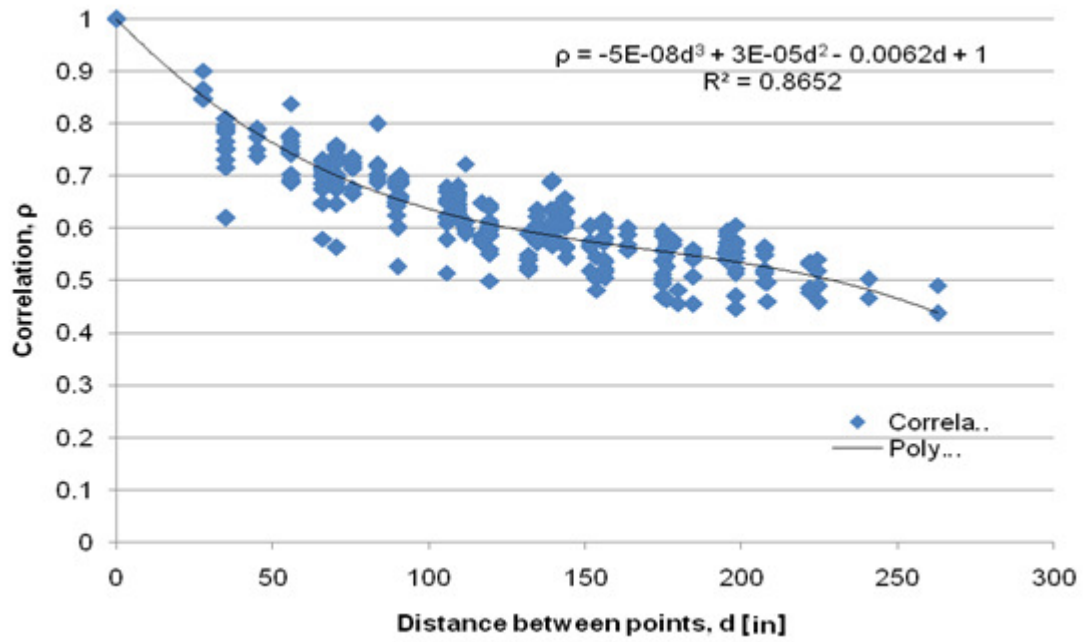


Figure 4.12: Development of correlation equation.

A portion of this matrix is shown in Figure 4.13, along with a corresponding map of the represented panels from Zone 2E. In accordance with the equation from Figure 4.12, there is a cubic relation between pressure correlation and distance between each panel. Correlation values for the complete structure ranged from 0.098 to 1.00.

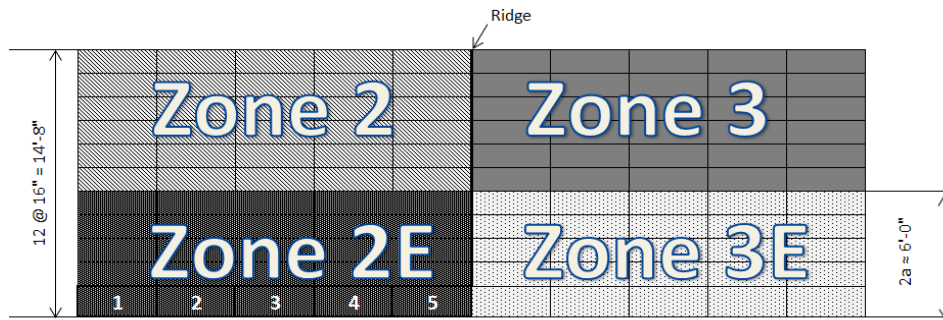
$$\begin{matrix}
 & \begin{matrix} 1 & 2 & 3 & 4 & 5 \end{matrix} \\
 \begin{matrix} 1 \\ 2 \\ 3 \\ 4 \\ 5 \end{matrix} & \begin{pmatrix}
 1 & 0.46 & 0.29 & 0.22 & 0.18 \\
 0.46 & 1 & 0.46 & 0.29 & 0.22 \\
 0.29 & 0.46 & 1 & 0.46 & 0.29 \\
 0.22 & 0.29 & 0.46 & 1 & 0.46 \\
 0.18 & 0.22 & 0.29 & 0.46 & 1
 \end{pmatrix}
 \end{matrix}$$


Figure 4.13: Excerpt from correlation matrix.

A pictorial representation of the matrix appears in Figure 4.14. Correlation curves have been plotted for the relative pressures on each panel relative to panel 1, located in the lower left-hand corner of the figure.

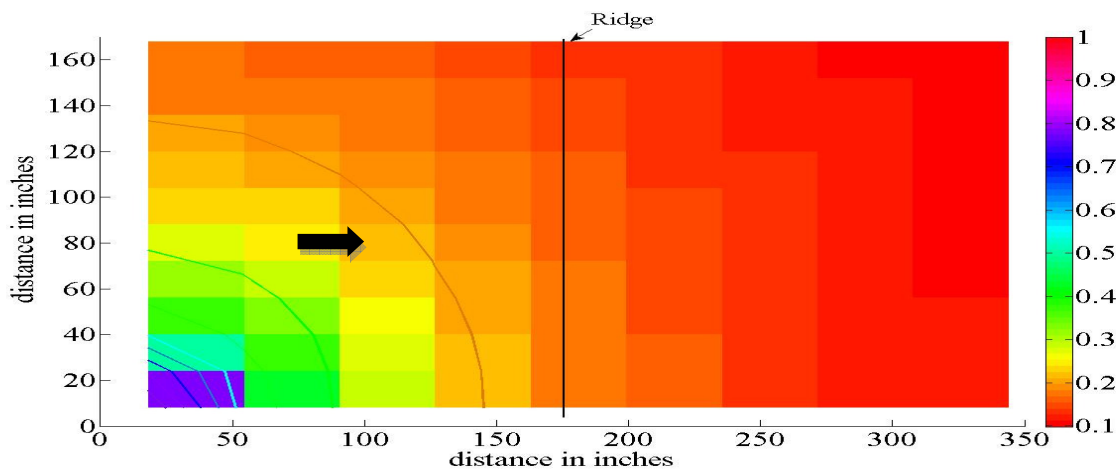


Figure 4.14: Correlation contours for all panels relative to panel 1.

Sample wind realizations

In conjunction with the statistical parameters presented in Table 4.1, the correlation matrix was used to generate random pressures for the sub-regions. Several of these are illustrated in Figures 4.15 and 4.16.

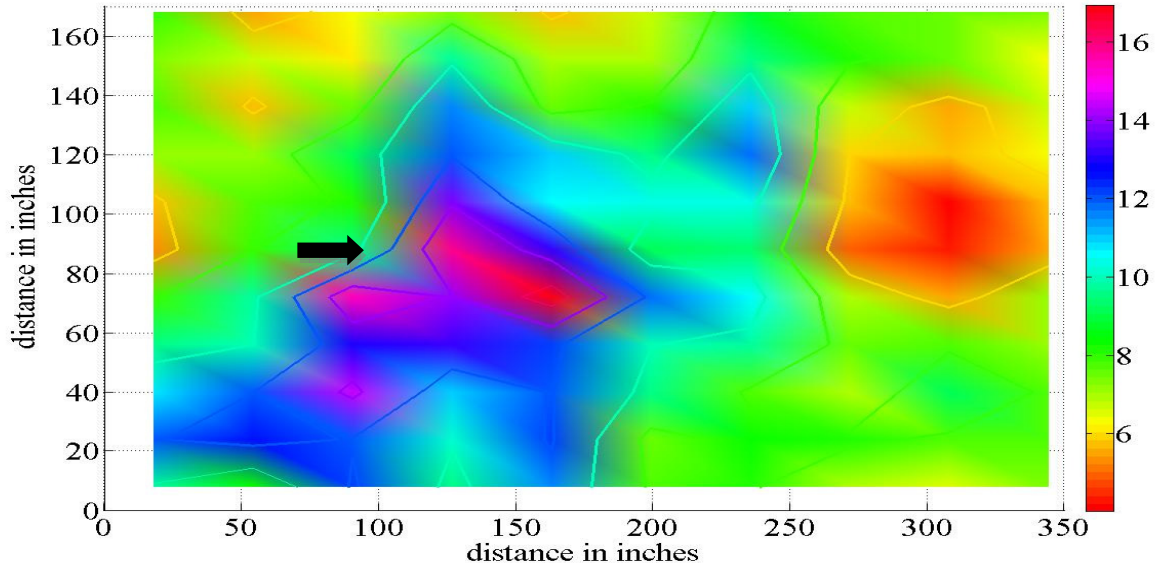


Figure 4.15: Sample wind realization with panel correlation #1 (psf).

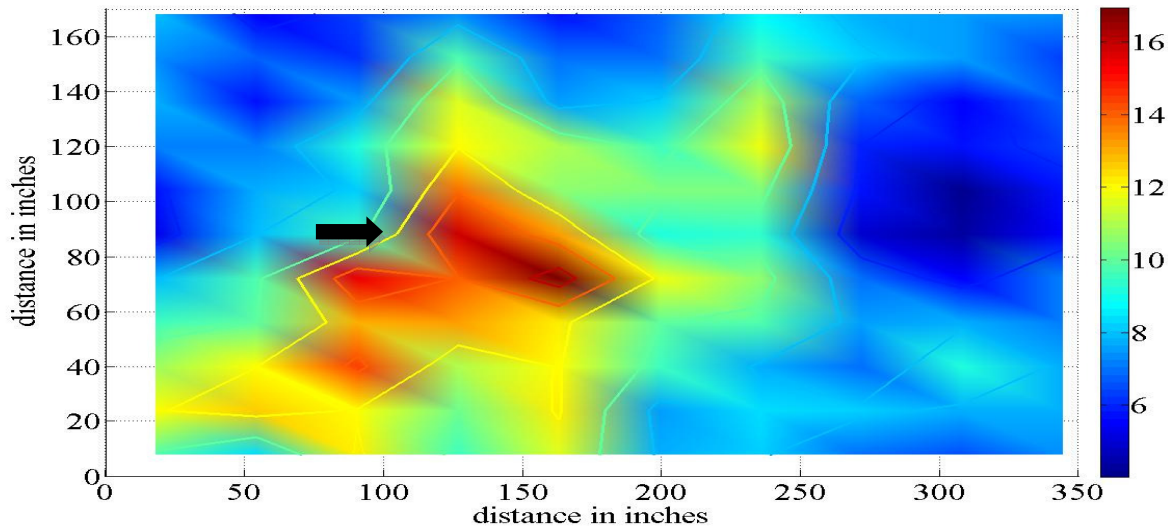


Figure 4.16: Sample wind realization with panel correlation #2 (psf).

Load Application

Only wind speeds of 100 mph and 130 mph perpendicular to the ridge were considered in this study. Random pressures were generated based on statistical information. Pressures were all assumed normal to the sheathing panel surface. It was assumed that the stiffness of a sheathing panel was relatively constant, and one-fourth of a panel's resultant load was distributed to each panel-rafter connection on the panel. This approach assumes that the sheathing is continuous over a large enough number of spans to validate the tributary area load distribution assumption. One should acknowledge that making specific conclusions about the internal forces in the sheathing is not justified under this loading approach. If internal sheathing forces are of concern, then distributed loads would need to be applied to the sheathing elements themselves – not their end nodes. Since the focus of this study is to explore the system behavior of the trusses and roof-to-wall connections, this simplified loading scheme is deemed appropriate. Further explanation of load application, simulations considered and the analysis performed is provided in Chapter Five.

CHAPTER FIVE

RELIABILITY

Fundamentals of Reliability

Structural verification is the process of checking the ability of a structure to resist applied loads. This process involves determining the loads to be applied, locations of these loads, how the loads are transmitted through the structure, the capacity of the structural members, and then comparing the applied load at any given location to the member's capacity at that point. In simple analysis and design, the values of load and resistance are treated as deterministic. Measuring the adequacy of a structure becomes as simple as comparing one number to another; if the load does not exceed the member's capacity, the design is valid.

As design codes have evolved, they have increasingly utilized a probabilistic approach. This is most evident in load factor resistance design (LRFD) provisions in the concrete, steel and wood design codes (AISC 2005; AFPA. 2005). This methodology recognizes the variability in loads and structural capacities, then attempts to account for them using modification coefficients in conjunction with probable load combinations. In this fashion, some of the random nature of these parameters can be addressed while maintaining the simplicity of the design equation.

Since actual values are not known, probability distributions are used to describe both demands and capacities. Without deterministic values, the criterion for determining

structural adequacy becomes more complicated. Instead of a simple comparison of the resistance value to the load, an equation is required:

$$G(x) = R(x) - L(x) \quad (5.1)$$

The function $G(x)$, known as a limit state function, is a way of formalizing the structural safety check whether one is dealing with deterministic values or not. The terms $R(x)$ and $L(x)$ represent the resistance (capacity) and load (demand) respectively as the random variables. When the demand exceeds the available resistance, $G(x)$ is less than zero, and the strength of the structure is inadequate. Similarly, when $G(x)$ is greater than zero, the structure has excess capacity and meets the design criterion. If the applied load is equal to the available capacity, $G(x) = 0$, the system is said to be at its limit state; the structure is satisfactory, but on the brink of failure (Melchers 1999).

The goal of reliability analysis is to determine the probability of violating a limit state during the service life of the structure while treating $L(x)$ and $R(x)$ as stochastic. The probability that the structure will fail in strength can be generally expressed as the probability that the limit state function will be less than zero (Melchers 1999):

$$P_f = P [G(R, L) \leq 0] \quad (5.2)$$

While designers typically check the strength of a structural element, they may also evaluate other aspects of the structure's performance, including serviceability issues. These non-structural criteria, such as allowable deflections or perceived accelerations, often govern the design. These requirements are subjective performance objectives. Other examples of performance objectives could be four adjacent connections not exceeding their axial capacities, shear stress does not surpass one-half of the ultimate stress for the

member, or all elements remain in their elastic regions. For simple probability distributions, determining this value mathematically is quite cumbersome and involves solving complex partial differential equations and evaluating convolution integrals (Melchers 1999). If the influencing variables' probability distributions functions are simple, the probability of violating the limit cannot be evaluated analytically. Hence, alternative means of ascertaining this quantity are often utilized.

Monte Carlo Simulation

Monte Carlo simulation is one common method of evaluating the probability of failure for more complex systems (Pinelli et al. 2004; Cramer et al. 2000; Sadek et al. 2004). This technique involves many sample tests (realizations), based on random values generated within the constraints of a given probability density function. One of the greatest advantages of this method is its applicability to any limit state without a significant change in required workload for more complicated problems. The probability of failure can be calculated as the number of realizations in which the limit state (I) was violated divided by the number of realizations completed (N):

$$P_f = I/N \quad (5.3)$$

Simulation yields only an approximation of the true value; the method's accuracy is dependent on the number of realizations. Equations are available to estimate the required number of realizations for a desired confidence level (Melchers 1999). Determining the

error within a simulation with a different number of realizations however, is not possible via equations. Determining relative accuracy can be assisted by plotting the probability of failure resulting from different numbers of realizations, as shown in Figure 5.1.

Eventually, the plot should converge to the actual value.

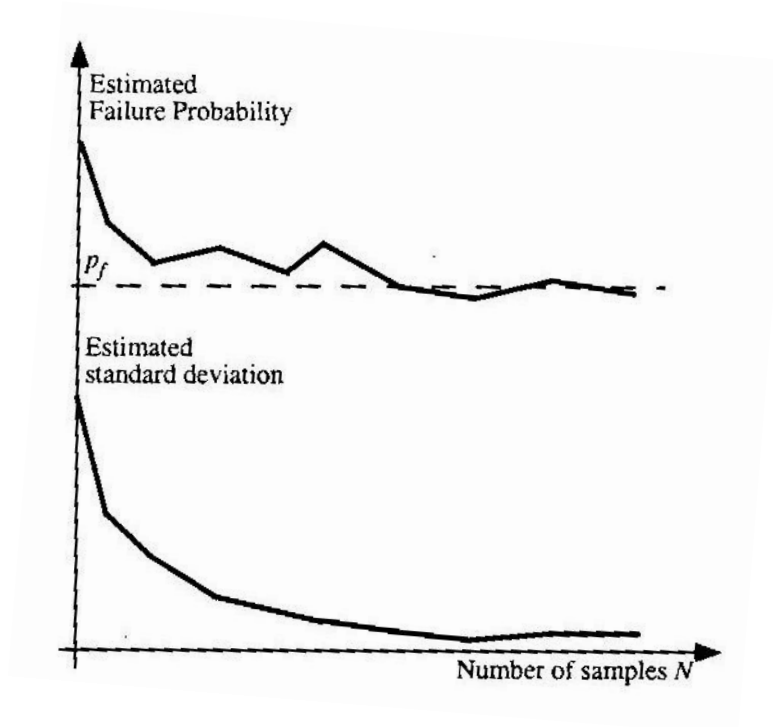


Figure 5.1: Typical convergence of probability estimate with increasing sample size (Melchers 1999).

Load Scenarios

This study evaluated six different load/modeling scenarios. Variables included wind pressure correlation, wind speed and roof-to-wall connection stiffness variability. Table 5.1 provides a summary of these scenarios. Wind speeds of 100 mph and 130 mph were used for each combination of correlation and stiffness conditions. A “panels” correlation indicates that each sub-region panel (Figure 4.7) has a different pressure value, but that

these values are governed by the correlation matrix from Chapter 4. In simulations without correlation, wind pressures were generated without considering the correlation matrix. Stiffness was either uniform for all connections or varied in accordance with the probability distribution presented in Table 3.1. The uplift capacity for each connection in the roof system is considered an independent random variable.

		wind pressure correlation	
		<i>none</i>	<i>panels</i>
connection stiffness	<i>variable</i>	NV	PV
	<i>uniform</i>	-	PU

Table 5.1: Simulation summary.

In reality, connection stiffness is variable and correlation of wind loads between roof panels is a good representation of actual conditions. One goal of this study is to identify the impact of incorporating these conditions in a reliability analysis of the roof system. The simulation scenarios outlined in Table 5.1 were carried out to determine if this level of refinement was necessary and, if so, the resulting effects on the probability of failure estimate.

Simulation Procedure

The basic procedure for each realization involved four main steps: 1) generating a random realization of the dead load, 2) generating a random wind pressure matrix, 3) gravity load analysis, and 4) wind load application. This section discusses the basic components of a given realization.

Load Generation

Each realization began with the generation of both dead loads and wind loads. The dead load in each simulation was assumed to be normally distributed with a mean of 10 psf and COV of 0.1 (Rosowsky and Cheng 1999a). A single dead load realization was assumed to be applicable to the entire roof structure. This load includes the weight of roof framing, sheathing and covering, which opposes the wind uplift load. Next, wind loads were generated for each panel based on correlation constraints for the given simulation and the lognormal probability distribution for pressures described in Table 4.1.

Analysis

The analysis phase of each realization commenced with the application of the dead load. After the entire dead load had been successfully applied to the structure, wind load application began. The nonlinear behavior of the connections and redistribution of load were captured by applying wind pressure in increments of 1/2000. After each load step, the number of connections exceeding the specified displacement, u_3 (Figure 3.7), was recorded. Loading continued in this fashion until the full load was applied to the structure or the model became numerically unstable.

Limit State

Past studies have assumed a variety of limit states for light-frame wood roof systems. One possible option is to use the failure of a single connection as the structural limit state, implying that the system fails if one connection's capacity is exceeded (Shanmugam et al. 2008). A recent study investigated a more parallel-system failure notion, using a limit state of four adjacent connections failing (Shamugam, Nielson and Gleason 2008). Specifically, this limit state assumes that the probability of five connections failing given that four connections have already failed is unity.

For this simulation, the performance criterion was one of structural stability. It was assumed that numerical instability corresponded to structural instability and represented a complete detachment of the roof system. This limit state was chosen to enable the investigation of connection failure patterns corresponding to various performance states, such as a definitive separation of the roof and wall, which might define a complete structural system failure.

Results

The results of the six simulations are presented in Table 5.2. Probabilities of failure range from 0.045 to 0.367, depending on simulation conditions. Recall that realizations were termed failures when the model became numerically unstable.

For a given set of stiffness and correlation conditions, the probability of failure of the system is generally nine times greater for a wind speed of 130 mph as compared to 100 mph. This agrees with expected results, as the uplift capacities of the nailed

connections modeled in this study are not very large. Once the initial static friction between the nail surface and the wood is overcome, pullout is only impeded by bending of the slanted nails. Since the uplift force applied to the connections is related to the square of the velocity (Equation 4.1), it follows that the increase in failure probabilities between wind speeds of 100 mph and 130 mph could be as different as seen in Table 5.2.

Simulation*	realizations	failures	P_f
PV100	3009	145	0.0482
PV130	1223	449	0.3671
PU100	1557	70	0.0450
PU130	1209	436	0.3606
NV100	1184	0	0.0000
NV130	1201	266	0.2215

*See Table 5.1

Table 5.2: Probabilities of failure.

Effect of Correlation

This study compared the effects of the correlation of wind pressures on adjacent roof panels to the results when no correlation constraints were applied. The primary goal was to investigate the effect of accounting for more local fluctuations over the roof than were included in the ASCE 7-05 wind design method. From Table 5.2, the probability of failure for correlated wind pressure with a velocity of 100 mph is 0.048, compared to 0.000 for non-correlated wind loads. A similar drop in probability of failure estimates exist between the panel-correlated and non-correlated wind pressures for a wind speed of 130 mph – 0.367 to 0.222 respectively.

At first glance, the results of NV100 (Table 5.2) may seem unlikely. However, upon further inspection, the fact that there was not a single failure within the 1184 realizations run seems reasonable. This particular simulation utilized variable connection stiffness values, but also did not consider correlation between the wind pressures applied at any point along the roof. Without correlation, it is entirely probable that neighboring wind pressures may have been generated such that they had largely different magnitudes. While these values would fit the probability distribution, the total demand on the rafter to wall connection for this realization would be lower than with correlated pressures. Therefore, it follows that not considering the correlation between wind pressures results in minimal failures.

Furthermore, assuming no correlation between wind pressures over the roof is not reasonable. In addition to accepted fluid mechanics laws (Cook 1985), further support for correlation is provided by the windPRESSURE data discussed in Chapter 3, which showed a minimum correlation of 0.098 between the farthest points on the system. This simulation corroborates the importance of considering correlation between the wind pressures across the roof, and serves as a baseline to compare other simulation results.

Effect of Variable Connection Stiffness

Past reliability analyses have not considered the inherent variation of connection stiffness within a structure (Rosowsky and Cheng 1999b). Due to the flexibility of the sheathing, load is distributed according to the relative stiffness of the connections. Table 5.2 suggests that considering this variable does not have a significant effect on the overall system reliability. The probability of failure for a 100 mph wind for uniform connection

stiffness was 0.0450. Including connection variability increases this value by 6.6% to 0.0482. Both simulations result in a reliability greater than 0.95. It should be noted that, although the NV and NU simulations had different numbers of realizations, this did not affect the predicted probability of failure much. Further discussion on this point is given later in the chapter.

Proposed Limit States

One of the biggest challenges in this field of research is determining appropriate limit states. There has been a number of studies that assumed the failure of one connection is identical to the failure of the system as a whole, a phenomenon termed a series system failure behavior (Shamugam et al. 2008). Recent work has proposed that system failure is dependent on multiple connections exceeding their capacities (Shamugam et al. 2008).

If series system failure behavior is truly what these systems exhibit, it stands to reason that the conditional probability of the second connection failing after the first has failed will be close to 1.0. Shanmugam et al. (2008) investigated the conditional probability of failure for four adjacent connections. Figure 5.2 shows that only for wind speeds of 150 mph or more does series system behavior appear to be valid. For lower wind speeds, the conditional probability of the second connection failing after the first is much lower than 1.0, refuting the series system claim.

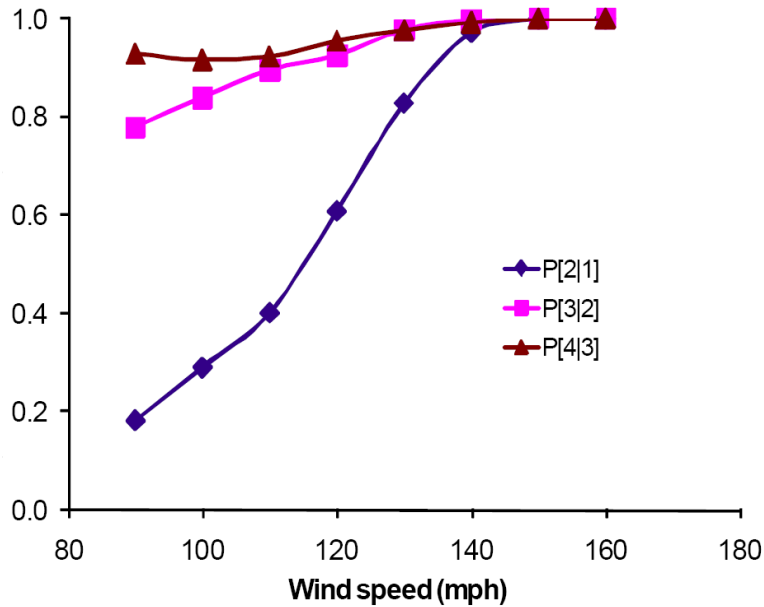


Figure 5.2: Conditional probabilities of failure (Shanmugam et al. 2008).

The current study determined the number of failed connections necessary for a system failure to occur. The number of failed connections for each failed realization was identified and the proportion of simulations meeting each failure condition is reported in Table 5.3. Simulation NV 100 is omitted from the table, as no realizations in this simulation failed. Recall that numerical instability was the only criterion by which system failure was determined. Connection failure is defined as the connection's displacement exceeding the displacement corresponding with its ultimate capacity (Figure 3.7).

number of failed connections	PU 100	PU 130	PV 100	PV 130	NV 130
0	1.000	1.000	0.985	0.883	0.895
1	0.000	0.000	0.000	0.031	0.034
2	0.000	0.000	0.000	0.020	0.030
3	0.000	0.000	0.000	0.047	0.015
4	0.000	0.000	0.015	0.007	0.019
5	0.000	0.000	0.000	0.007	0.008
6	0.000	0.000	0.000	0.004	0.000

Table 5.3: Ratio of failed connections in failed realizations.

With over 88% of the realizations failing before a single connection could fail independently, these results may provide strong support for the series failure assumption. Further investigation was conducted for realizations failing with zero connections past their failure displacement. The ratios of carried force to ultimate capacity for each connection in these realizations were inspected to determine how close the connections were to failure. If several connections had a force ratio very close to 1.0, simultaneous failure on the subsequent load step would have been a feasible explanation for why so many system realizations failed before the failure of any individual connection. Table 5.4 shows the proportion of connections whose ratios of carried force to ultimate force were at or above 0.95.

number of connections within 0.5% of failure load	PU 100	PU 130	PV 100	PV 130	NV 130
0	0.986	0.861	0.955	0.735	0.759
1	0.014	0.028	0.015	0.086	0.128
2	0.000	0.010	0.008	0.061	0.060
3	0.000	0.028	0.015	0.052	0.023
4	0.000	0.033	0.008	0.025	0.030
5	0.000	0.020	0.000	0.020	0.000
6	0.000	0.020	0.000	0.020	0.000

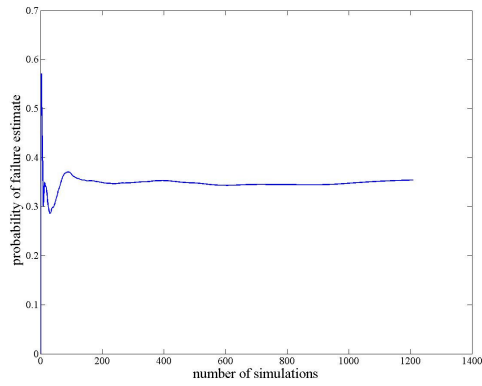
Table 5.4: Proportion of connections within five percent of failure in failed realizations.

Of the failed realizations, only 1.4 to 16.5 percent the simulations had between 1 and 6 connections close enough to their capacities to reasonably assume they may have failed on the subsequent load step. This recognition leads to some doubt regarding the applicability of the limit state utilized.

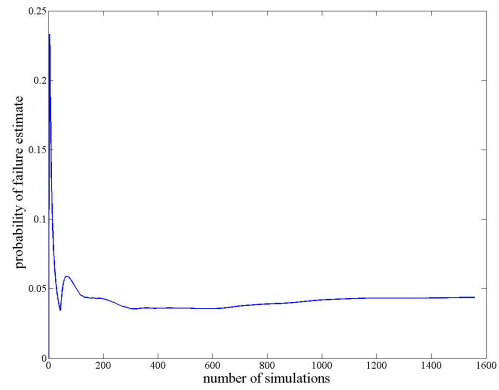
Evaluation of Accuracy

After review of these results, it is apparent that the limit state utilized in this study (numerical instability) may not have been the most appropriate. The reader is reminded that limit states are completely subjective and, in this case, may have been arbitrary. Although the limit state may not have been appropriate, the study was conducted accurately enough to give the results some meaning. Moreover, the primary objective of this research was to develop and propose a method for ascertaining the reliability of the roof system.

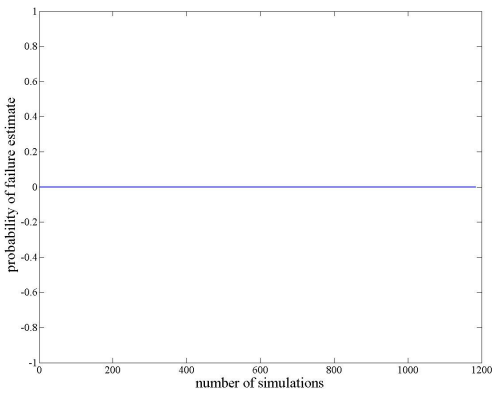
As shown in Figure 5.1, the relative accuracy of a given number of simulations can be determined by plotting the probability of failure resulting from different numbers of realizations. Such plots were generated for each of the six simulations, and appear in Figures 5.3. Since each plot appears to converge on a probability of failure, these plots confirm that a sufficient number of samples were used in each simulation.



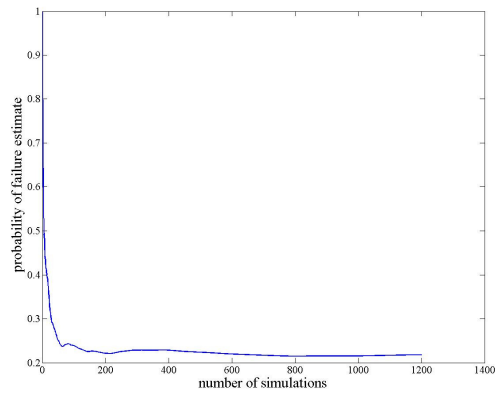
(a) PV 100



(b) PV 130

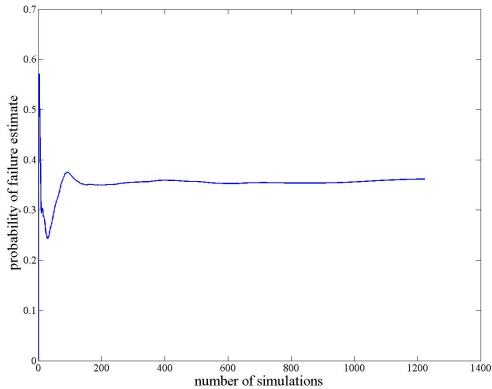


(c) NV 100

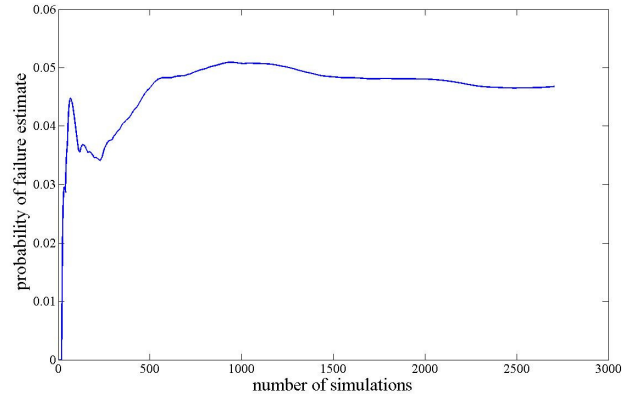


(d) NV 130

Figure 5.3: Probability of failure versus number of realizations.



(e) PU 100



(f) PU 130

Figure 5.3 (cont.): Probability of failure versus number of realizations.

Fragility Curves

Fragility curves are the graphical representation of probability of failure data. Figure 5.4 shows the extrapolated curves based on the results of the current study. While only two data points per curve limits the accuracy, these curves can show general trends in the failure probabilities for the different condition at various wind speeds. As seen in the figure, the structural behavior appears to be very similar for both PV and PU conditions, while the failure probability for NV conditions is lower for all speeds. Table 5.5 shows the median wind speed values for each extrapolated curve. These wind speeds, which range from 139.0 mph to 147.8 mph, correspond with an estimate probability of failure of 50%.

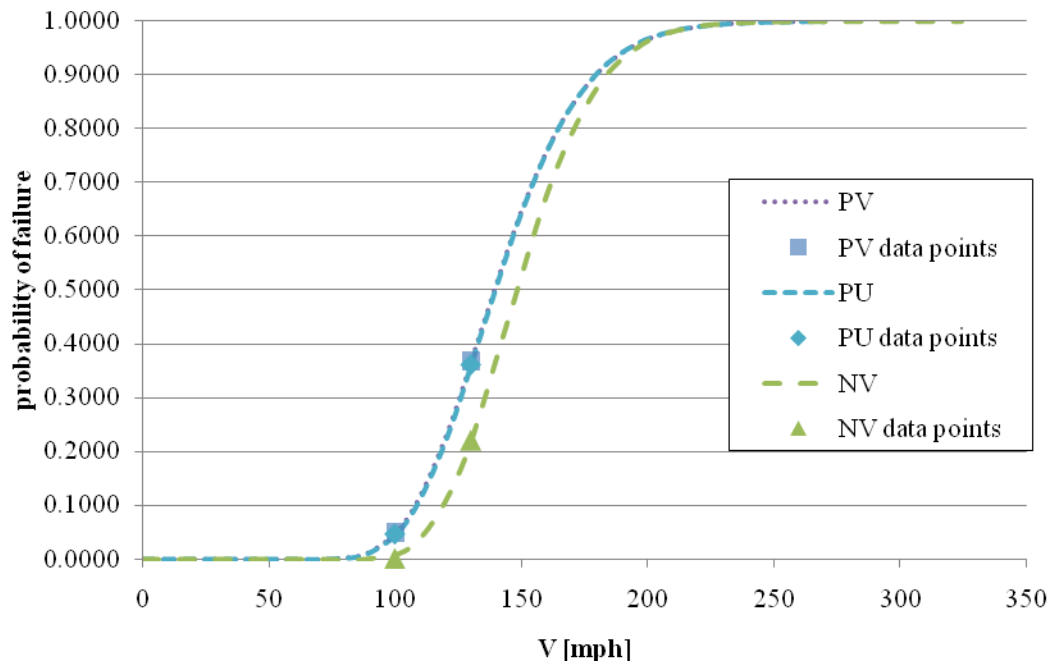


Figure 5.4: Extrapolated fragility curve (illustration only).

Simulation	Median V [mph]
PV	139
PU	139.4
NV	147.8

Table 5.5: Median wind speeds.

CHAPTER SIX

CONCLUSIONS

This study aimed to address two major objectives: to determine the influence of inherent variability in the properties of key components on roof system behavior and to develop and propose an enhanced method for determining the reliability of a roof system typical to low-rise residential wood construction under wind loads. Both of these objectives were achieved. The influence of key components' properties considered in this study was limited to the roof-to-wall connections and the wind correlation. In particular, variable connection stiffness was explored. Utilizing analytical models for various aspects of the wind loaded structure, a method for determining reliability was developed.

Effect of Variable Stiffness on System Reliability

The influence of variable stiffness on the system reliability was determined to be insignificant. A variation in connection stiffness should alter the load distribution and redistribution paths, leading to increased load on stiffer connections due to the flexibility of the diaphragm and an increased failure rate since connection capacity was still modeled as a random variable. The probability of failure for simulations in which the connection stiffness was uniform was lower than those with variable connection stiffness. However, the difference between probabilities of failure was within 0.007 for both wind speeds, a relatively insignificant difference. It is possible that the sheathing may have behaved as a rigid diaphragm or that the connection stiffness' probabilistic distribution is

not wide enough for significant variability to occur. However, a more probable explanation for these results is that the assumed limit state of numerical instability was not entirely appropriate for this simulation.

Proposed Method for Evaluating System Reliability

The structural model, wind correlation matrix and simulation techniques explained in this document provide a basic framework for evaluating the reliability of a low-rise wood frame roof system under wind loads.

A structural model capable of portraying system behavior must first be generated. This study provides a basic model that can be easily utilized in future studies. One of the most prominent features of the model is the utilization of the roof-to-wall connection analytical model (Shanmugam et al. 2009) to capture the nonlinear behavior observed in in-situ structures. Had the model been created in a commercial package, such as SAP2000 (Computers and Structures 2006), it would not have had as significant nonlinear modeling capabilities. Using OpenSees (McKenna 2009) as the platform, however, enables researchers without access to commercial programs to utilize the model and also provides sufficient nonlinear analysis capability.

Next, a method for ascertaining the loads must be selected. This study utilized parameters suggested by past research efforts in the probabilistic distributions for both dead and wind loads. It is recommended that this practice be followed in subsequent studies. The major contribution of this research was a reasonable method for capturing the spatial variation of the wind. While this study utilized existing data to determine an

equation for the correlation of pressures with respect to distance, the underlying principle was that wind tunnel data can be used to generate a correlation matrix of wind pressures. This matrix, in conjunction with past research regarding the statistical parameters of wind load, can be used to generate wind loads that are in agreement with the known spatial correlation.

In order to determine a probability of failure, a failure criterion in the form of a limit state must be selected. Numerical instability, which was chosen for this study, does not seem to be an ideal choice. Future work should investigate this further.

Finally, Monte Carlo simulation can be used to determine the probability of failure of the system. Care must also be taken to run a sufficient number of realizations. To ensure an adequate number of realizations were run, this study utilized a probability estimate with respect to sample number plot (Figure 5.3). Had the probability of failure not converged, additional realizations would have been required.

This procedure was utilized in generating the probability of failure for the six different systems described in Chapter Five. The simulations run in this research generated a variety of preliminary results that will assist in further studies.

Recommendations for Future Work

This project was a good preliminary step in determining the reliability of low-rise wood frame roof systems. The simulation methods outlined provide a reasonable way of accounting for the spatial variation of wind and nonlinear behavior of the roof-to-wall

connection. There are many possible avenues for the continuation and improvement of this research.

Although a preliminary method for determining wind loads was proposed, several aspects of this method would benefit from further study. It is recommended that the level of correlation be investigated. Only two levels of correlation, no correlation and partial correlation between 39.11" x 16" panels, were explored in this study. ASCE 7-05 zones assume full correlation over all points in a particular zone. It would be very interesting to see how the probability of failure changes with the size of wind zones and to determine how small of an area is necessary to capture the effects of the wind's spatial variation.

Other methods of determining the wind load's statistical distribution should also be considered. This study calculated the statistical parameters using ASCE 7-05 main wind force resisting system (MWFRS) wind loads. Since the focus is on determining an appropriate discretization level, wind load values should reflect the smaller application areas. One method for doing this would be to use the components and cladding provisions in ASCE 7. While these estimated values are appropriate for use in design, using more precise data might be appropriate. Wind tunnels studies could be performed to generate data for this purpose. Such data could also be utilized in generating the correlation matrix. Instead of generating an interpolation function from scaled data points, perhaps actual wind tunnel data could be examined, and a correlation matrix determined from it.

It is envisioned that, eventually, the model will be expanded to include not only the roof system, but the entire structural system of the house. Perhaps a model can be

generated from in-situ data for the sheathing-to-rafter connections like the one between the rafters and top plate. Non-structural elements, such as shingles and siding could also be added.

The method illustrated in this study has the potential to be used to generate fragility curves for the roof system in light-frame residential wood structures. These curves would illustrate the probability the system will fail for a given wind loading (Figure 6.1). Many more simulations, with various wind speeds and directions, would be required to generate such curves. Various limit states could also be considered so that, ultimately, this fragility information could be used to assess the probability of a particular failure mode for these systems given some return period.

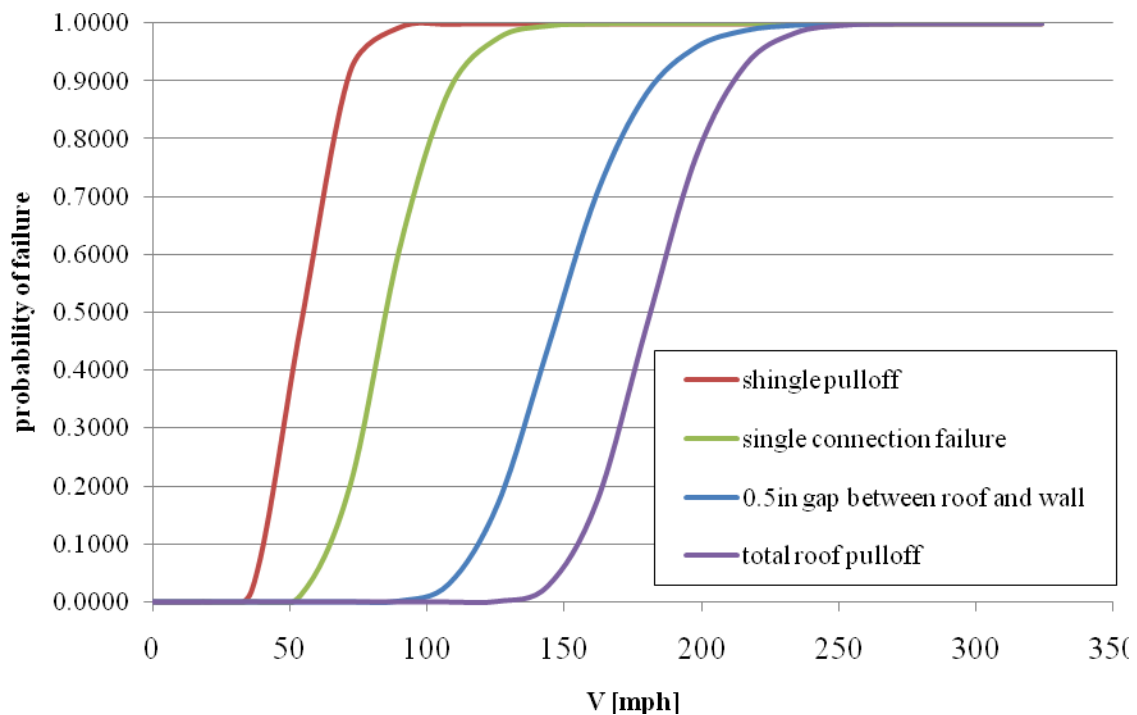


Figure 6.1: Fragility curves for multiple limit states (illustration only).

Fragility curves would be useful to multiple agencies, as they highlight the probability that a structure will fail under various conditions. Such knowledge is beneficial to insurance companies when deciding whether or not to insure a structure and for how much. Fragility curves could also be utilized by FEMA, particularly in their HAZUS-MH program. They provide a valid basis for risk assessment of residential homes subjected to high winds. Fragility curves may also be utilized to assess the effectiveness of connection failure mitigation strategies, such as retrofitting.

Additionally, knowing the probability of failure for a particular connection type can provide a basis for changing building codes. One of the largest potential payoffs of this project would be the eventual use of this method and model in generating results that could be used to revise the building codes governing light frame coastal wood construction.

REFERENCES

- American Forest & Paper Association, Inc. ASD/LRFD Manual for Engineered Wood Construction, 2005.
- American Forest & Paper Association, Inc. Design Values for Wood Construction: Revised Supplement to the Revised 1991 Edition of NDS. Washington, DC:, 1993.
- American Institute of Steel Construction. Steel Construction Manual. 13th ed., 2005.
- American Society of Civil Engineers. ASCE 7-05: Minimum Design Loads for Buildings and Other Structures.
- Blake, Eric S., Edward Rappaport, and Christopher W. Landsea. The Deadliest, Costliest and most Intense United States Tropical Cyclones from 1851 to 2006 (and Other Frequently Requested Hurricane Facts). Vol. NOAA Technical Memorandum NWS TPC-5., 2007. 3/13/08 <<http://www.nhc.noaa.gov/pdf/NWS-TPC-5.pdf>>.
- "California Uses HAZUS-MH to Reassess Safety of Hospitals." February 27, 2008 2008. FEMA. <http://www.fema.gov/plan/prevent/hazus/eq_ca_hospitals.shtm>.
- Cheng, Jim. "Testing and Analysis of the Toe-Nailed Connection in the Residential Roof-to-Wall System." Forest Products Journal 54.4 (2004): 58-65. .
- Computers and Structures, Inc. ETABS. Vol. 9. Berkeley, CA:, 2005.
- Computers and Structures, Inc. SAP2000. Vol. 10.0.4/1. Berkeley, CA:, 2006.
- Cook, N. J. The Designer's Guide to Wind Loading of Building Structures: Part 1. England: Butterworth-Heinemann, 1985.
- Cramer, Steven M., John M. Drozdek, and Ronald W. Wolfe. "Load Sharing Effects in Light-Frame Wood-Truss Assemblies." Journal of Structural Engineering 126.12 (2000): 1388-94.
- Criswell, M. E. "Response of Realistic Wood Joist Floors." Probabilistic Mechanics and Structural Reliability (1979): 156.
- Davidson, Rachel A., Huan Zhao, and Vineet Kumar. "Quantitative Model to Forecast Changes in Hurricane Vulnerability of Regional Building Inventory." Journal of Infrastructure Systems 9.2 (2003): 55-64.

- Ellingwood, Bruce R., et al. "Fragility Assessment of Light-Frame Wood Construction Subjected to Wind and Earthquake Hazards." Journal of Structural Engineering 130.12 (2004): 1921.
- Ellingwood, Bruce R., and Paulos Beraki Tekie. "Wind Load Statistics for Probability-Based Structural Design." Journal of Structural Engineering 125.4 (1999): 453-64.
- Endo, M., B. Bienkiewicz, and H. J. Ham. "Wind-Tunnel Investigation of Point Pressure on TTU Test Building." Journal of Wind Engineering and Industrial Aerodynamics 94.7 (2006): 553-78.
- FEMA. HAZUS-MH. Federal Emergency Management Agency. Vol. M3., 2007.
- Folz, Bryan, and Ricardo O. Foschi. "Reliability-Based Design of Wood Structural Systems." Journal of Structural Engineering 115.7 (1989): 1666-80. .
- Gupta, R. 1. "System Behaviour of Wood Truss Assemblies." Progress in Structural Engineering and Materials 7.4 (2005): 183-93.
- Holmes, J. Wind Loading of Structures. 1st ed. New York, New York: Spon, 2001.
- Hunt, D. "Kite Flying Around Wind Obstacles." Kaper 2005.
- Jarrell, Jerry D., Max Mayfield, and Edward Rappaport. The Deadliest, Costliest, and Most Intense United States Hurricanes From 1900 to 200 (and Other Frequently Requested Hurricane Facts). Vol. NWS TPC-1. Miami, FL: NOAA/NWS/Tropical Prediction Center, 2001. 10/04/08.
- Keith, Edward L., and John D. Rose. "Hurricane Andrew - Structural Performance of Buildings in South Florida." Journal of Performance of Constructed Facilities 8.3 (1994): 178-91. .
- Lee, Kyung Ho, and David V. Rosowsky. "Fragility Assessment for Roof Sheathing Failure in High Wind Regions." Engineering Structures 27.6 (2005): 857-68.
- Lindt, van De, et al. "Performance of Wood-Frame Structures during Hurricane Katrina." Journal of Performance of Constructed Facilities 21.2 (2007): 108-16.
- Main, Joseph A. WindPRESSURE., 2006.
- Melchers, Robert E. Structural Reliability Analysis and Prediction. Ed. John Wiley & Sons, Ltd. 2nd ed. England: John Wiley & Sons, Ltd., 1999.

- Mtenga, P. V., et al. "System Factors for Light-Frame Wood Truss Assemblies." Journal of Structural Engineering 121.2 (1995): 290-300.
- NASA. "Re-Living the Wright Way." 11 April 2008. <<http://wright.nasa.gov/>>.
- Pielke, Roger A., Jr, and Christopher W. Landsea. "Normalized Hurricane Damages in the United States: 1925-95." Weather and Forecasting 13.3 (1998): 621-31. .
- Pinelli, Jean-Paul, et al. "Hurricane Damage Prediction Model for Residential Structures." Journal of Structural Engineering 130.11 (2004): 1685-91.
- Pourzeynali, Saeid, and T. K. Datta. "Reliability Analysis of Suspension Bridges Against Fatigue Failure from the Gusting of Wind." Journal of Bridge Engineering 10.3 (2005): 262-71.
- Reed, T. D., D. V. Rosowsky, and S. D. Schiff. "Uplift Capacity of Light-Frame Rafter to Top Plate Connections." Journal of Architectural Engineering 3.4 (1997): 156-63.
- Rosowsky, David V., and Ningqiang Cheng. "Reliability of Light-Frame Roofs in High-Wind Regions. I: Wind Loads." Journal of Structural Engineering 125.7 (1999a): 725-33.
- Rosowsky, David V., and Ningqiang Cheng. "Reliability of Light-Frame Roofs in High-Wind Regions. II: Reliability Analysis." Journal of Structural Engineering 125.7 (1999b): 734-9.
- Rosowsky, David V., and Bruce R. Ellingwood. "Performance-Based Engineering of Wood Frame Housing: Fragility Analysis Methodology." Journal of Structural Engineering 128.1 (2002): 32-8.
- Rosowsky, David V., Thomas D. Reed, and Kenneth G. Tyner. "Establishing Uplift Design Values for Metal Connectors in Light-Frame Construction." Journal of Testing & Evaluation 26.5 (1998): 426-33. .
- Rosowsky, David V., and Guangren Yu. "Partial Factor Approach to Repetitive-Member System Factors." Journal of Structural Engineering 130.11 (2004): 1829-41.
- Sadek, Fahim, et al. "Sampling Errors in the Estimation of Peak Wind-Induced Internal Forces in Low-Rise Structures." Journal of Engineering Mechanics 130.2 (2004): 235-9.
- Shanmugam, B., B. G. Nielson, and D. O. Prevatt. "Statistical and Analytical Models for Roof Components in Existing Light-Framed Wood Structures." (2009).

Shamugam, B., B. G. Nielson and D. O. Prevatt. "Probabilistic Descriptions of in-Situ Roof to Top Plate Connections in Light Frame Wood Structures." ASCE Structures Congress. Vancouver, BC, Canada, April 24-26, 2008.

Shamugam, B., B. G. Nielson and A. Gleason. "Fragility Assessment of Light-Framed Wood Roof System Subject to High Wind Loads." Inaugural International Conference of the Engineering Mechanics Institute. Minneapolis, MN, May 18-21, 2008.

MathWorks. MATLAB. Vol. 7.6., 2008.

Sparks, Peter R., and Shiraj A. Bhinderwala. "Relationship between Residential Insurance Losses and Wind Conditions in Hurricane Andrew." (1994): 111. .

McKenna, F., and G. Fenves. OpenSees. Version 2.1.0., 2009.

Tieleman, H. W., Zhongfu Ge, and M. R. Hajj. "Theoretically Estimated Peak Wind Loads." Journal of Wind Engineering and Industrial Aerodynamics 95.2 (2007): 113-32.

van der Hoven, Isaac. "T1 Power Spectrum of Horizontal Wind Speed in the Frequency Range from 0.0007 to 900 Cycles Per Hour." J. Atmospheric Sciences 14.2 (1958): 160. . 28 Feb 2009

Vickery, Peter J., et al. "HAZUS-MH Hurricane Model Methodology. II: Damage and Loss Estimation." Natural Hazards Review 7.2 (2006): 94-103.

Yin, Yue-Jun. Correlation Coefficient Matrix of Wind Pressure Coefficient. Michigan Technological University, 2009. (unpublished)